UNIMORE
UNIVERSITÀ DEGLI STUDI DI
MODENA E REGGIO EMILIA

Università degli studi di Modena e Reggio Emilia

Dipartimento di Scienze Fisiche, Informatiche e Matematiche
Laurea Magistrale in Matematica

Mathematical Modelling of Koalas' Home Range

Primo Relatore:
Prof.ssa Cecilia Vernia

Secondo Relatore:
Prof. Federico Frascoli

Candidata:
Francesca Montorsi

Anno accademico 2024/2025

Contents

Introduction

The advent of radiotelemetry in the late 1950s radically changed the study of animal movements. It allows researchers to obtain accurate measurements of animal relocations at fixed intervals and thus to track them in their habitat. These data are fundamental to define and estimate the home range, the space use of an individual during its normal activities, including foraging, dispersal, and mating. We can distinguish two different classes of approach: the statistical method and the mechanistic method. The first offers only a descriptive estimate of the pattern of space use and it provides a summary of relocation data, which results in a loss of biological realism.It fails to predict the actual distribution of the animal and its statistical methods often struggle with outliers. For instance, the widely adopted Minimum Convex Polygons (MCP) method is sensitive to outliers; it is not able to weight the observations differently because its algorithm does not follow any probabilistic structure. MCP defines the home range with a convex polygon that encloses all the points collected, or a percentage of it (usually 95%), whether they are located in the core area, or isolated far from the majority of the observations. Moreover, it does not account for the frequency of relocations and treats all data as equally important regardless of their density. To overcome these issues, the statistical Fixed Kernel method has been developed. First, the algorithm considers each collected point as a kernel probability density function with peak centred at that point and then sums these kernels to obtain a smooth density estimate that represents the probability of space use, known as the Utilization Distribution (UD). From this probability function, specific percentages (commonly the 95%, 75%, or 50% so-called "isopleths") can be extracted to identify the spatial boundaries and the intensity of use within different zones of animal home range.

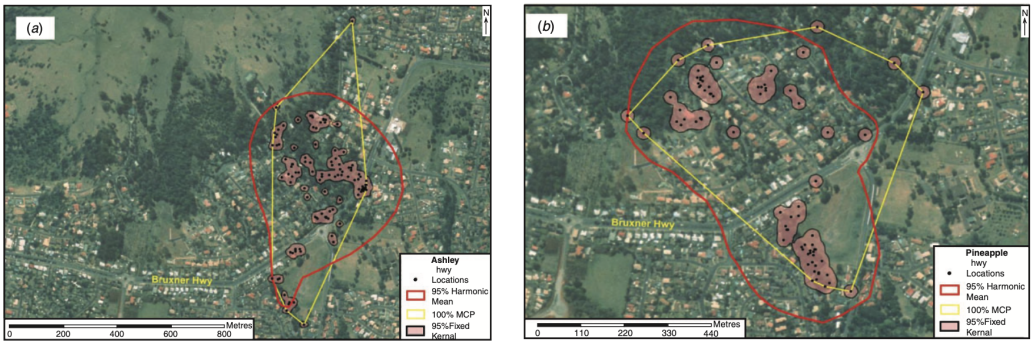

Figure 1: Comparison between MCP and KDE estimation of space use of two koalas, (a) Ashley and (b) Pineapple, in an urban area of north-east New South Wales

Mechanistic methods provide an alternative to purely statistical estimators. They have been used to study movements of cells, microorganisms (Brown and Berg, 1974; Alt, 1980; Palsson and Othmer, 2000) and insects (Kareiva and Shigesada, 1983), but limited studies of vertebrate dynamics have been conducted. Mechanistic methods provide an estimate of the actual pattern of space use and derive spatial distribution of individuals through particular mathematical formulations. These formulations are defined by specific parameters, that reflect the underlying rule of animal movements; hence, their selection is fundamental for obtaining an accurate prediction of the evolution of an ecosystem. Mechanistic methods yield the basis for developing a predictive theory of animal spatial dynamics, which is particularly crucial for the conservation of iconic species like the koala, a native species of Australia. In our study in particular, we analyse and estimate a koala home range with a mechanistic method, solving a system of advection-diffusion equations.
Currently, we can find koala populations on the east and south coast of Australia, specifically in New South Wales (NSW), Queensland and Victoria (Fig. 3). The genetic diversity across each population is fundamental to maintain the biodiversity of the species as it is an adaptation to different habitats. Koala populations on the east coast (NSW and East Queensland) are classified as an endangered species due to severe habitat fragmentation caused by urban development; however, island populations, such as those on French Island, Victoria, and North Stradbroke Island, Queensland, are facing issues of koala overabundance and biologists aim to mitigate the growth of that population (Fig. 2). On these islands, koalas have shown low genetic diversity because they have been isolated from other populations and protected from various diseases for generations. Thus, relocating these koalas to the mainland could have a more negative than positive impact, for example contributing to the spread of diseases like Chlamydia. Consequently, in this

Figure 2: French Island, November 2025

specific case, a deeper understanding of the social structure and home ranges of these populations is crucial to guarantee their survival.

Given the lack of specific natural predators, the spatial dynamic of the koalas is primarily governed by other factors, such as habitat quality, mating, and proximity to urban areas. Koalas prefer a fertile habitat as it provides trees with leaves richer in nutrients. They sleep most of the day and are active at night; they are generally solitary and tend to avoid conspecifics, particularly in low-density areas. Moreover, koalas typically do not exhibit aggressive behaviour outside of the breeding season, often allowing for overlap in space use with other individuals. However, these social dynamics change during the mating and breeding season, which runs from October to January and peaks in late October. During this period, male-male interactions are characterized by territorial fights for access to female home ranges. A single male typically focuses its attention on one or two females simultaneously, although it is possible for a male, in a high density population, to have interactions with up to five females during the breeding season, as has been recorded in Cape Otway, Victoria (Watchorn and Whisson, 2019). The overabundance of koalas in such areas results in smaller home ranges with a high probability of overlap. This condition is a threat to both animal and vegetation species and can lead to canopy defoliation and eventually to mass starvation of the population.

Nevertheless, even in stable environments, these spatial dynamics can be modified by anthropogenic factors. For instance, the effects of short-term disturbances on koalas' home range areas have been analysed by Phillips (2016), who investigated how disruptive was a five-day music festival in northern

NSW in April 2010. Seven Koalas with home ranges adjacent to the festival area were monitored to observe their behavioural responses. The study shows that loud acoustic disturbance caused alterations in koalas' spatial dynamics, specifically for individuals living within 525 m of the staging area. Three Koalas exhibited an evacuation of their home range during the active days of festival, but they eventually returned to their original core areas after the concert. Other koalas, whose home range was far away up to 725 m from the staging area, modified their movement in the opposite direction of the noise, but they remained in their ranging boundaries. Even though most of the individuals returned to their original home ranges after the festival, the acoustic disturbance had a great impact on the stress of koalas. It is documented that a high level of cortisol can suppress the immune system and this could increase susceptibility to disease, most notably Chlamydiosis, thus even short-term disturbances can have ecological consequences that persist in the long term.

While the acoustic disturbances have primarily psychological effects on koalas and consequently provide an alteration in movement directions, as a behavioural response, the urbanisation of koala habitat has a direct physical impact. Artificial infrastructures, such as roads, railways and fences, fragment the space use creating structural constraints on koalas' movement and this leads to a modification on home range size and shape. Moreover, these anthropogenic constructions are considered as a primary cause of population decline in regions such as New South Wales and Queensland. Koalas living in urbanised areas are at higher risk of vehicle collisions, domestic dog attacks, and starvation due to the loss of natural habitat.

The size and shape of koalas' home range vary with respect to resource availability, population density and the presence of anthropogenic barriers. For instance, the home ranges of koalas in some areas are delimited by infrastructure and roads. This fragmentation is a primary cause of koala deaths and alteration of behaviour. In Redland City, Queensland, seven koalas were monitored for up to 28 weeks during the breeding season in 2009 to analyse the impact of linear infrastructure (De Oliveira et al., 2014). Statistically, the home ranges in this urbanised area were larger than those previously measured in the same region. This may be the effect of forcing the koalas to travel longer distances through isolated forest patches in search for food and mates. For most of the tracked individuals in that study, fences and railways were used as boundaries for their ranging areas. The high mortality rate observed, three deaths in seven monitored koalas caused by train strikes and domestic dog attacks, dramatically shows the great responsibility of urban development in population decline. Therefore, it is vital to investigate koala responses to urban development and to define strategies to mitigate this

decline.
All these social and environmental factors define koala's home range, which can be effectively studied with mathematical mechanistic models based on advection diffusion equations.

Figure 3: Spatial distribution of Koalas, 2007 (Mcalpine et al.)

The aim of this study is to adapt the mechanistic framework, described in available literature existing for mathematical ecology for wolves and other canids, (Moorcroft and Lewis, 2006), to analyse koalas' movement patterns. Specifically, we investigate the probability density function of two koalas occupying the same domain, by employing a system of advection-diffusion equations, which allow us to analyse the possibility of interaction and overlap of animals' home ranges. In particular, Chapter 1 reviews the analytical formulation of the advection-diffusion equation and its application to different species, such as wolves and passerines. In Chapter 2, we study numerical steady-state solutions of the advection-diffusion system that describes the movement dynamics of two koalas in a one-dimensional space. Finally, Chapter 3 reviews the analytical steady-state solutions of the same system and explores numerical solutions for the non linear PDEs advection-diffusion system. A final chapter concludes this study with a discussion and several ideas for future developments.

Chapter 1

Literature Review and origin of the advection-diffusion equations

1.1 Definition of the advection-diffusion equation

We consider a probability density function $u(x,t)$ that must describe the probability density of finding a koala at position x at time t. It is defined as follows:

$$u(x,t+\tau) = \int_{-\infty}^{\infty} u(x',t)k(x',x,\tau,t)dx', \tag{1.1}$$

where τ represents the time step from one observation to another, x is the one-dimensional location at time $t+\tau$ and x' is the location at time t. We call the displacement, at each time step, $a := (x - x')$, and we assume that the direction and length of the displacement depend only on the starting location x'.
The function $k(x', x, \tau\ , t)$ is the redistribution kernel, which describes the probability that an individual located at the interval $[x', x' + dx]$ at time t will move to a position between $[x, x + dx]$ at time $t + \tau$.
Expanding the right-hand side of the equation (1.1) using a Taylor series and letting $dx, \tau \to 0$ we can obtain the expression for the advection-diffusion equation, in one dimension:

$$\frac{\partial u}{\partial t} = \frac{\partial^2}{\partial x^2}(du) - \frac{\partial}{\partial x}(cu),$$

where d and c are the diffusion and the advection coefficients respectively.
Let us see this in detail. First, it's useful to reparametrise the integral in terms of a and x, hence not explicitly of x'.

Performing a simple substitution

$$x' = x - a \Longrightarrow da = -dx',$$

we have

$$u(x, t+\tau) = \int_{-\infty}^{\infty} u(x-a, t)k(x-a, a, \tau\ , t)da. \tag{1.2}$$

The integrand has the following expansion with respect to the variable x:

$$\begin{aligned} u(x-a,t)k(x-a,a,\tau,t) = u(x,t)k(x,a,\tau\ ,t)+ \\ + \sum_{m=1}^{\infty} \frac{(-a)^m}{m!} \frac{\partial^m}{\partial x^m}(u(x,t)k(x,a,\tau,t)). \end{aligned}$$

Substituting this expansion in the Eq. (1.2) we find:

$$\begin{aligned} u(x, t+\tau) = \int_{-\infty}^{\infty} \Bigg[u(x,t)k(x,a,\tau\ ,t)+ \\ + \sum_{m=1}^{\infty} \frac{(-a)^m}{m!} \frac{\partial^m}{\partial x^m}(u(x,t)k(x,a,\tau,t)) \Bigg] da. \end{aligned} \tag{1.3}$$

Since the redistribution kernel represents a probability density transition, its integral must satisfy:

$$\int_{-\infty}^{\infty} k(x, a, \tau, t)da = 1.$$

It is easy to check that

$$\int_{-\infty}^{\infty} u(x,t)k(x,a,\tau,t)da = u(x,t).$$

Therefore, Eq. (1.3) becomes

$$\begin{aligned} u(x, t+\tau) = u(x,t) + \int_{-\infty}^{\infty} \Bigg(-a\frac{\partial}{\partial x}(u(x,t)k(x,a,\tau,t))+ \\ + \frac{a^2}{2}\frac{\partial^2}{\partial x^2}(u(x,t)k(x,a,\tau,t)) \Bigg) da+ \\ + \int_{-\infty}^{\infty} \left(\sum_{m=3}^{\infty} \frac{(-a)^m}{m!} \frac{\partial^m}{\partial x^m}(u(x,t)k(x,a,\tau,t)) \right) da. \end{aligned}$$

Assuming that the integrand satisfies the hypothesis of Fubini's theorem, we move the derivatives outside the integral. Since $u(x,t)$ is independent from a, it is also factored out. Furthermore, the non-integral terms are shifted to the left side of the equation and then the entire equation is divided by τ. This leads to:

$$\begin{aligned}\frac{u(x,t+\tau)-u(x,t)}{\tau} = &-\frac{1}{\tau}\frac{\partial}{\partial x}\left(u(x,t)\int_{-\infty}^{\infty} ak(x,a,\tau,t)da\right)+\\ &+\frac{1}{2\tau}\frac{\partial^2}{\partial x^2}\left(u(x,t)\int_{-\infty}^{\infty} a^2k(x,a,\tau,t)da\right)+\\ &+\frac{1}{\tau}\sum_{m=3}^{\infty}\frac{(-1)^m}{m!}\frac{\partial^m}{\partial x^m}\left(u(x,t)\int_{-\infty}^{\infty} a^mk(x,a,\tau,t)da\right).\end{aligned}$$

For small τ, $(\tau \to 0)$, the equation reduces to:

$$\begin{aligned}\frac{\partial u(x,t)}{\partial t} = &\lim_{\tau\to 0}-\frac{1}{\tau}\frac{\partial}{\partial x}\left(u(x,t)\int_{-\infty}^{\infty} ak(x,a,\tau,t)da\right)+\\ &+\lim_{\tau\to 0}\frac{1}{2\tau}\frac{\partial^2}{\partial x^2}\left(u(x,t)\int_{-\infty}^{\infty} a^2k(x,a,\tau,t)da\right)+\\ &+\lim_{\tau\to 0}\frac{1}{\tau}\sum_{m=3}^{\infty}\frac{(-1)^m}{m!}\frac{\partial^m}{\partial x^m}\left(u(x,t)\int_{-\infty}^{\infty} a^mk(x,a,\tau,t)da\right).\end{aligned} \tag{1.4}$$

According to Pawula's theorem we can state that the truncated version of Eq. (1.4) is the Fokker-Planck equation, which has only two terms of the sum, $(m = 1, 2)$ and the other coefficients with $m > 2$ are zero. Specifically, the theorem states that for a positive transition probability k, the expansion may stop after the first or second term; otherwise it must contain an infinite number of terms.
Thus, we obtain the advection-diffusion equation as follows:

$$\begin{aligned}\frac{\partial}{\partial t}u(x,t) = &-\lim_{\tau\to 0}\frac{1}{\tau}\frac{\partial}{\partial x}\left(u(x,t)\int_{-\infty}^{\infty} ak(x,a,\tau,t)da\right)+\\ &+\lim_{\tau\to 0}\frac{1}{2\tau}\frac{\partial^2}{\partial x^2}\left(u(x,t)\int_{-\infty}^{\infty} a^2k(x,a,\tau,t)da\right),\end{aligned}$$

or, in other words,

$$\frac{\partial}{\partial t}u(x,t) = -\frac{\partial}{\partial x}(c(x,t)u(x,t)) + \frac{1}{2}\frac{\partial}{\partial x}(d(x,t)u(x,t)),$$

where

$$c(x,t) = \lim_{\tau \to 0} \frac{1}{\tau} \int_{-\infty}^{\infty} ak(x,a,\tau,t)da$$

and

$$d(x,t) = \lim_{\tau \to 0} \frac{1}{2\tau} \int_{-\infty}^{\infty} a^2 k(x,a,\tau,t)da$$

represent the first and second moments of the distribution of movement predicted by the kernel k, as $\tau \to 0$.
In order to have the dependency of c and d with respect to the variables x and x', we can substitute $a = (x - x')$ and thus:

$$c(x,t) = \lim_{\tau \to 0} \frac{1}{\tau} \int_{-\infty}^{\infty} (x - x')k(x',x,\tau,t)dx',$$

$$d(x,t) = \lim_{\tau \to 0} \frac{1}{2\tau} \int_{-\infty}^{\infty} (x - x')^2 k(x',x,\tau,t)dx'.$$

A similar procedure allows us to obtain higher-order equations. To accurately capture the spatial dynamics of animal species and give a more realistic representation of home range formation, it is often necessary to extend this framework to a two-dimensional space. In the next section we discuss this transition by generalising the displacement and the advective parameter into vectorial quantities.

1.1.1 Two-dimensional Advection-Diffusion equation

The equation (1.1) in two dimensions becomes

$$u(\mathbf{x}, t+\tau) = \int_{-\infty}^{\infty} \int_{-\infty}^{\infty} u(\mathbf{x}', t)k(\mathbf{x}', \mathbf{x}, \tau\ , t)dx'dy'$$

where $\mathbf{x} = (x, y)$ is a two dimensional vector that corresponds to the location of an individual at time t and $k(\mathbf{x}', \mathbf{x}, \tau, t)d\mathbf{x}d\mathbf{x}'$ is the probability of an individual to move from a rectangle $d\mathbf{x}'$ at time t to a rectangle $d\mathbf{x}$ at time $t + \tau$. We call the displacement, at each time step, $\mathbf{a} := \mathbf{x} - \mathbf{x}'$, which is now a vectorial quantity. Consequently, the advective parameter c is generalised into a two-dimensional vector $\mathbf{c} = (c_x, c_y)$.
Analogously to the approach applied in 1D advection-diffusion equations, assuming the direction and length of the displacement depend only on the starting point $\mathbf{x}'$, we expand the integrand using its Taylor series truncated at the second order, as shown below. We find:

$$u(\mathbf{x},t)\ k(\mathbf{x},\mathbf{a},\tau\ ,t) = u(\mathbf{x},t)\ k(\mathbf{x},\mathbf{a},\tau\ ,t) - \mathbf{a}^T\ \nabla_x \cdot (u(\mathbf{x},t)k(\mathbf{x},\mathbf{a},\tau,t))+$$
$$+\frac{1}{2}\ \mathbf{a}^T\ H_{uk}(\mathbf{x},t)\ \mathbf{a}$$

with $H_{uk}(\mathbf{x},t)$ being the Hessian matrix of uk. Therefore, the advection-diffusion equation becomes:

$$\begin{aligned}\frac{\partial}{\partial t}u(\mathbf{x},t) = -\nabla\cdot(\mathbf{c}(\mathbf{x},t)u(\mathbf{x},t)) + \frac{\partial^2}{\partial x^2}(d_{xx}(\mathbf{x},t)u(\mathbf{x},t))+ \\ + \frac{\partial^2}{\partial x\partial y}(d_{xy}(\mathbf{x},t)u(\mathbf{x},t)) + \frac{\partial^2}{\partial y\partial x}(d_{yx}(\mathbf{x},t)u(\mathbf{x},t))+ \\ + \frac{\partial^2}{\partial y^2}(d_{yy}(\mathbf{x},t)u(\mathbf{x},t))\end{aligned} \tag{1.5}$$

where

$$\mathbf{c}(\mathbf{x},t) = \lim_{\tau\to 0}\frac{1}{\tau}\int_{-\infty}^{\infty}\int_{-\infty}^{\infty}(\mathbf{x}-\mathbf{x}')k(\mathbf{x}',\mathbf{x},\tau\ ,t)d\mathbf{x}', \tag{1.6}$$

$$d_{xx}(\mathbf{x},t) = \lim_{\tau\to 0}\frac{1}{2\tau}\int_{-\infty}^{\infty}\int_{-\infty}^{\infty}(x-x')^2k(\mathbf{x}',\mathbf{x},\tau\ ,t)d\mathbf{x}', \tag{1.7}$$

$$d_{xy}(\mathbf{x},t) = d_{yx}(\mathbf{x},t) = \lim_{\tau\to 0}\frac{1}{2\tau}\int_{-\infty}^{\infty}\int_{-\infty}^{\infty}(x-x')(y-y')k(\mathbf{x}',\mathbf{x},\tau\ ,t)d\mathbf{x}', \tag{1.8}$$

$$d_{yy}(\mathbf{x},t) = \lim_{\tau\to 0}\frac{1}{2\tau}\int_{-\infty}^{\infty}\int_{-\infty}^{\infty}(y-y')^2k(\mathbf{x}',\mathbf{x},\tau\ ,t)d\mathbf{x}'. \tag{1.9}$$

In our case we assume that successive relocations of koalas are recorded sufficiently close in time to understand their movements but far enough apart to be independent from each other. This means that the covariance between two successive relocations is zero; consequently, since d_{xy}, d_{yx} represent the covariance, we set $d_{xy}(\mathbf{x},t) = d_{yx}(\mathbf{x},t) = 0$. Moreover, we consider an isotropic diffusion, implying that koalas' random movements are uniform in all directions. Therefore we can simplify the diffusive terms to a unique $d(\mathbf{x},t)$, obtaining the following equation:

$$\frac{\partial}{\partial t}u(\mathbf{x},t) = -\nabla\cdot(\mathbf{c}(\mathbf{x},t)u(\mathbf{x},t)) + \nabla^2\cdot(d(\mathbf{x},t)u(\mathbf{x},t)). \tag{1.10}$$

The coefficients $\mathbf{c}(\mathbf{x}, t)$ and $d(\mathbf{x}, t)$ are known as advection and diffusion coefficients, respectively, reflecting their physical origin.
In order to explain their origins and meanings, let us introduce two particular redistribution kernels, corresponding respectively to directed and random movements. These are observed for the case of an individual moving at constant speed, with relocations recorded at fixed time interval.
Examining the case of directed motion, first, we consider a redistribution kernel k for $(\mathbf{x} - \mathbf{x}')$, defined as a delta function as follows:

$$k(\mathbf{x}', \mathbf{x}, \tau\ , t) = \delta(\mathbf{x}' - \mathbf{x} - \gamma\tau\hat{\boldsymbol{\alpha}}), \tag{1.11}$$

where γ is a constant speed of movement, $\hat{\boldsymbol{\alpha}}$ is a unit vector pointing in the fixed direction of movement and τ is the fixed time step at which every relocation is made. Here $\mathbf{x}'$ and $\mathbf{x}$ are the location observed at time t and the successive time step $(t+\tau)$ respectively. In other words, this kernel describes the movement of an individual moving from one location to another in a straight line.
We want to show that this kernel, with the probability density function u, produces only one non-zero coefficient, and it is equal to advection coefficient, $\mathbf{c}$, in Eq. (1.10).
Indeed, if we substitute this kernel into the equation (1.6)-(1.9), we obtain:

$$\begin{aligned}\mathbf{c}(\mathbf{x}, t) &= \lim_{\tau\to 0}\frac{1}{\tau}\int_{-\infty}^{\infty}\int_{-\infty}^{\infty}(\mathbf{x} - \mathbf{x}')\delta(\mathbf{x}' - \mathbf{x} - \gamma\tau\hat{\boldsymbol{\alpha}})\, d\mathbf{x}' = \\ &= \lim_{\tau\to 0}\frac{1}{\tau}\gamma\tau\hat{\boldsymbol{\alpha}} = \gamma\hat{\boldsymbol{\alpha}},\end{aligned} \tag{1.12}$$

$$\begin{aligned}d_{xx}(\mathbf{x}, t) + d_{yy}(\mathbf{x}, t) &= \lim_{\tau\to 0}\frac{1}{2\tau}\int_{\mathbb{R}^n}|\mathbf{x}' - \mathbf{x}|^2\delta(\mathbf{x}' - \mathbf{x} - \gamma\tau\hat{\boldsymbol{\alpha}})\, d\mathbf{x}' \\ &= \lim_{\tau\to 0}\frac{1}{2\tau}\gamma^2\tau^2 = \lim_{\tau\to 0}\frac{1}{2}\gamma^2\tau = 0.\end{aligned} \tag{1.13}$$

Under the assumption of isotropic diffusion, and given that d_{xx} and d_{yy} must be positive, Eq. (1.13) implies that they must both be zero for $\tau \to 0$.
Analogously to the case above, we assume $d_{yx} = d_{xy} = 0$ for $\tau \to 0$.
This means that if we substitute these equations for $\mathbf{c}$ and d_{ij} in (1.10) it simplifies as a pure advection equation:

$$\frac{\partial}{\partial t}u(\mathbf{x}, t) = -\nabla\cdot(\mathbf{c}(\mathbf{x}, t)u(\mathbf{x}, t)) = -\nabla\cdot(\gamma\vec{\mathbf{x}}u) = -\gamma\vec{\mathbf{x}}\cdot\nabla u. \tag{1.14}$$

A kernel that corresponds to directed movements, such as the one defined in (1.11), describes the actual trajectory and relocations of an individual. However, if we consider animals moving in random directions at each time step, the resulting path provides only an approximation rather than an exact representation of the underlying trajectory. The accuracy of the path corresponding to this kernel increases as time step decreases, but it has to be large enough to guarantee the independence between successive relocations. Thus, sampling uncorrelated relocations, we obtain a distribution of movement that estimates the redistribution kernel k.
As we have seen previously, the advection term $\mathbf{c}(\mathbf{x}, t)$ represents the average distance travelled from one location to the other in one time step, and since the individual has not preferred direction, the mean value in this case is zero.

$$\mathbf{c}(\mathbf{x}, t) = \frac{1}{\tau}\frac{1}{n_r - 1}\sum_{i=0}^{n_r-1}(\mathbf{x}_{i+1} - \mathbf{x}_i) = 0$$

where $\mathbf{x}_{i+1} - \mathbf{x}_i$ is the distanced moved from one location, at time t, to the successive one, at time $t + \tau$. The number of steps is n_r.
On the other hand, the diffusion term $d(\mathbf{x}, t)$ is represented by the mean square displacement of successive relocations in the x and y directions per unit time τ and this is always positive. This means:

$$d_{xx}(\mathbf{x}, t) = \frac{1}{2\tau}\frac{1}{n_r - 1}\sum_{i=0}^{n_r-1}(x_{i+1} - x_i)^2 > 0$$

and

$$d_{yy}(\mathbf{x}, t) = \frac{1}{2\tau}\frac{1}{n_r - 1}\sum_{i=0}^{n_r-1}(y_{i+1} - y_i)^2 > 0.$$

In this case, Eq. (1.10) reduces to a purely diffusive expression:

$$\frac{\partial}{\partial t}u(\mathbf{x}, t) = \nabla^2 \cdot (d(\mathbf{x}, t)u(\mathbf{x}, t)). \tag{1.15}$$

These examples explain well the origin of the terms in the advection-diffusion equation, e.g.:

$$\frac{\partial}{\partial t}u(\mathbf{x}, t) = \underbrace{-\nabla \cdot (\mathbf{c}(\mathbf{x}, t)u(\mathbf{x}, t))}_{\substack{\text{Advection}\\ \text{(directed motion)}}} + \underbrace{\nabla^2 \cdot (d(\mathbf{x}, t)u(\mathbf{x}, t))}_{\substack{\text{Diffusion}\\ \text{(random motion)}}}. \tag{1.16}$$

Finding an analytical solution to this equation is only possible for specific cases and often quite complex. In Chapter 3 we derive a steady state solution for cases of interest in the dynamics of Koalas in one-dimensional settings.

1.1.2 A kernel $k(x', x, \tau, t)$ with localising tendency

Systems of advection-diffusion equations as defined in Eq. (1.16) have been used to study and predict the movements of animals, including wolves and coyotes, and how they can coexist in neighbouring habitats and avoid territorial conflicts. Studies have shown that a uniform redistribution kernel k is not sufficient to describe those movements because an important behavioural tendency is missing. Hence, it is necessary to introduce a more refined kernel that could take into account animals' localising tendency, or the tendency to move towards specific areas of interest for various reasons.
A similar behaviour has also been observed in koalas especially during breeding season. They tend to remain for continuous periods in the same area, allowing their home ranges to overlap with those of other koalas, until they need to move and search for a more suitable area to create a new home range. Thus, we can conclude that a uniform redistribution kernel does not correspond to an advection diffusion equation which can predict koalas movement and home range, as it applies, although for different reasons, to canides and birds.
Let us now include this localising tendency in the definition of the redistribution kernel k. We consider a redistribution kernel k, corresponding to a random walk with attraction towards a particular area of interest, expressed as a product of two different distributions: $f_\tau(\rho)$, which describes the probability of an individual to move from $\mathbf{x}'$ to $\mathbf{x}$, and the $K(\phi, \hat{\phi})$ that refers to the localising tendency of the individual, or the probability of moving in the ϕ direction toward a particular area.
The relocations of individuals are made from $\mathbf{x}'$ to $\mathbf{x}$, the distance between them is given as $\rho = |\mathbf{x}' - \mathbf{x}|$ and all the locations are associated with two different angles: $\phi = \tan^{-1}\left(\dfrac{y - y'}{x - x'}\right)$ and $\hat{\phi} = \tan^{-1}\left(\dfrac{y}{x}\right)$. In other words, ϕ is the angle between the two relocations $\mathbf{x}'$ and $\mathbf{x}$, while $\hat{\phi}$ is the one between $\mathbf{x}$ and the area of interest, which we suppose coincides with the origin, for simplicity.
From these definitions we have the following derivations:

$$\cos(\hat{\phi}) = \frac{x}{|\mathbf{x}|}, \qquad \sin(\hat{\phi}) = \frac{y}{|\mathbf{x}|},$$

$$\cos(\phi) = \frac{x - x'}{|\mathbf{x} - \mathbf{x}'|}, \qquad \sin(\phi) = \frac{y - y'}{|\mathbf{x} - \mathbf{x}'|},$$

$$\cos(\phi - \hat{\phi}) = \frac{\mathbf{x}}{|\mathbf{x}|} \cdot \frac{\mathbf{x} - \mathbf{x}'}{|\mathbf{x} - \mathbf{x}'|}, \qquad \sin(\phi - \hat{\phi}) = \frac{(-y, x)^T}{|\mathbf{x}|} \cdot \frac{\mathbf{x} - \mathbf{x}'}{|\mathbf{x} - \mathbf{x}'|}.$$

The last two definitions are derived from the others using the double sine and cosine formulas. Now, if we consider a redistribution kernel as defined above, where the turning kernel K is an even function of $(\phi - \hat{\phi})$, we can obtain an expression for c and d, i.e. the advection and diffusion coefficients. Observing that the movements of individuals are not explicitly dependent on time, we can drop this dependency in our calculations and use the general expressions (1.6)-(1.9) for c and d_{ij} to substitute the definition of $k = f_\tau(\rho)K_\tau(\phi, \hat{\phi})$ in them.
Thus we obtain

$$\mathbf{c}(\mathbf{x}) = \lim_{\tau\to 0} \frac{1}{\tau} \int_0^{2\pi} \int_0^{\infty} (\mathbf{x} - \mathbf{x}') f_\rho(\rho) K(\phi - \hat{\phi}) d\rho d\phi, \tag{1.17}$$

$$d_{xx}(\mathbf{x}) = \lim_{\tau\to 0} \frac{1}{2\tau} \int_0^{2\pi} \int_0^{\infty} (x - x')^2 f_\rho(\rho) K(\phi - \hat{\phi}) d\rho d\phi, \tag{1.18}$$

$$d_{yy}(\mathbf{x}) = \lim_{\tau\to 0} \frac{1}{2\tau} \int_0^{2\pi} \int_0^{\infty} (y - y')^2 f_\rho(\rho) K(\phi - \hat{\phi}) d\rho d\phi. \tag{1.19}$$

The vector $\mathbf{c}(\mathbf{x})$ points directly towards the site of interest and it has no component perpendicular to that direction. Indeed, since K is assumed to be even and $\sin(\phi - \hat{\phi})$ is odd, the vector product between $\mathbf{c}$ and the vector orthogonally pointing to the origin $\dfrac{(y, -x)^T}{|\mathbf{x}|}$ must be zero. On the other hand, the product between $\mathbf{c}$ and the vector pointing towards the area of interest $\dfrac{\mathbf{x}}{|\mathbf{x}|}$ is not necessarily zero.
We explicitly have:

$$\begin{aligned} -\mathbf{c}(\mathbf{x}) \cdot \frac{\mathbf{x}}{|\mathbf{x}|} &= \lim_{\tau\to 0} \frac{1}{\tau} \int_0^{2\pi} \int_0^{\infty} |\mathbf{x} - \mathbf{x}'| \frac{\mathbf{x} - \mathbf{x}'}{|\mathbf{x} - \mathbf{x}'|} \cdot \frac{\mathbf{x}}{|\mathbf{x}|} f_\rho(\rho) K(\phi - \hat{\phi}) d\rho d\phi = \\ &= \lim_{\tau\to 0} \frac{1}{\tau} \int_0^{\infty} \rho f_\rho(\rho) d\rho \int_0^{2\pi} \cos(\phi - \hat{\phi}) K(\phi - \hat{\phi}) d\phi \end{aligned}$$

and

$$\begin{aligned} -\mathbf{c}(\mathbf{x}) \cdot \frac{(y, -x)^T}{|\mathbf{x}|} &= \lim_{\tau\to 0} \frac{1}{\tau} \int_0^{2\pi} \int_0^{\infty} |\mathbf{x} - \mathbf{x}'| \frac{\mathbf{x} - \mathbf{x}'}{|\mathbf{x} - \mathbf{x}'|} \cdot \frac{(y, -x)^T}{|\mathbf{x}|} f_\rho(\rho) \cdot \\ &\quad \cdot K(\phi - \hat{\phi}) d\rho d\phi = \\ &= \lim_{\tau\to 0} \frac{1}{\tau} \int_0^{\infty} \rho f_\rho(\rho) d\rho \int_0^{2\pi} \sin(\phi - \hat{\phi}) K(\phi - \hat{\phi}) d\phi = 0. \end{aligned}$$

Studies have shown that taking $f_\tau(\rho)$ as an exponential and $K(\phi - \hat{\phi})$ as a von Mises Distribution, we can reproduce an accurate prediction of wolves and coyotes home ranges, while they are moving with localising tendency toward their den site. A von Mises distribution is the circular version of the Gaussian distribution and it is defined as follows:

$$K(\phi, \hat{\phi}) := \frac{1}{2\pi I_0(k_v)} e^{k_v \cdot cos(\phi - \hat{\phi})}$$

where $I_0(k_v)$ is the modified Bessel function of first kind of zeroth order which normalises K to integrate to 1; $\hat{\phi}$ is the mean direction of individual movements of the animal or group of animals considered and $k_v \geq 0$ represents the concentration parameter of $I_0(k_v)$ and it defines the degree of uniformity of K. The distribution becomes increasingly non-uniform as the magnitude of k_v increases, reducing to a uniform distribution when $k_v = 0$.

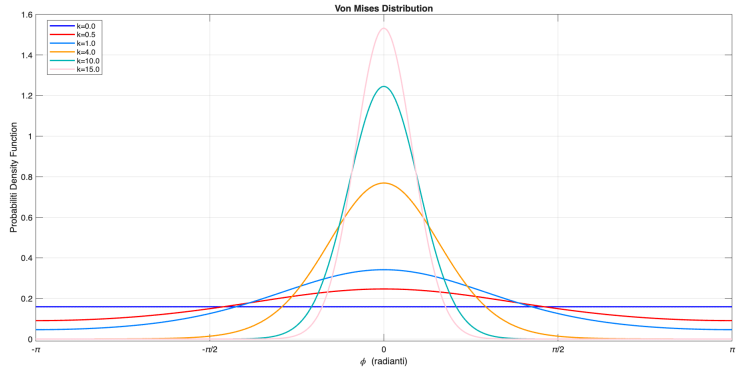

Figure 1.1: Von Mises Distribution with different concentration parameters

1.2 Typical advection-diffusion equation for canids and birds

To obtain an analytically tractable model, we now reduce the two-dimensional territorial system to a one-dimensional steady-state problem, retaining only the key effects of conspecific avoidance and diffusion.

1.2.1 Advection-diffusion for two packs of wolves

As demonstrated by several studies, (Holgate, 1971; Peters and Mech, 1978; Okubo et al., 2001), and described mathematically in "Mechanistic home range analysis" by Lewis and Moorcroft, wolves and many other carnivores

do not show uniform movement patterns. Their movements reflect their needs depending on various factors, such as landscape features, food availability, avoidance of interactions with other packs, and seasonal breeding. Data collected by tracking wolf packs show that their space use increases rapidly at a certain time of the year but then it stabilises over a long period corresponding to the breeding season. During those times, wolves movements tend to remain around the den in order to keep their pups safe, to forage for food and avoid interactions with other packs.
Wolves movements can be decomposed in two main contributions: a directed component toward the centre of the home range and a random component associated with foraging. The tendency toward the den site is driven by the environmental scents that other animals leave behind. Individuals leave olfactory trails for various reasons, most notably territorial defense and mate attraction. Scent marks are essential for predators, like wolves, to define the boundary and to reduce aggressive encounters with conspecific rivals. Consequently, wolves home ranges exhibit a higher density of scent mark in correspondence with their boundaries.
For example, let us consider two packs of wolves, U and V, moving in a two dimensional space domain. We also take into account their avoidance tendency with respect to foreign scent marks, respectively $p(\mathbf{x}, t)$ and $q(\mathbf{x}, t)$, which are defined as follows:

$$\frac{\partial p}{\partial t}(\mathbf{x}, t) = Nu(\mathbf{x}, t)(l + mq(\mathbf{x}, t)) - \mu p(\mathbf{x}, t),$$

and

$$\frac{\partial q}{\partial t}(\mathbf{x}, t) = Nv(\mathbf{x}, t)(l + mp(\mathbf{x}, t)) - \mu q(\mathbf{x}, t),$$

where N is the number of individuals in each pack, l and μ represent the scent marking rate without any foreign scent marks and the decay rate, respectively. Moreover, m denotes the sensitivity of marking response to foreign scent marks.
With respect to the previous paragraph, in order to define the von Mises distribution that produces an accurate model of the home ranges of wolf packs, we define the concentration parameters k_τ^u and k_τ^v. They give the degree of uniformity of the distributions K_u and K_v as follows:

$$k_\tau^u = b\overline{\rho}_\tau q(\mathbf{x}, t),$$

$$k_\tau^v = b\overline{\rho}_\tau p(\mathbf{x}, t).$$

Here $\overline{\rho}_\tau$ represents the average displacement of wolves in one time step τ and b reflects the sensitivity of the distribution of movement directions to foreign scent marks. This means that the uniformity of distributions K^u and K^v is governed by the product of the parameter b and the densities of scent marks $p(\mathbf{x}, t)$ and $q(\mathbf{x}, t)$ from the other pack. Following the same approach we used to obtain Eq. (1.10), we can derive the expression for c and d:

$$c = \lim_{\tau \to 0} \frac{b\overline{\rho}_\tau}{2\tau}, \qquad\qquad d = \lim_{\tau \to 0} \frac{\overline{\rho}_\tau^2}{4\tau}.$$

Thus, the equations for packs' densities $u(\mathbf{x}, t)$, $v(\mathbf{x}, t)$ are given by:

$$\frac{\partial}{\partial t} u(\mathbf{x}, t) = -c\nabla \cdot (u(\mathbf{x}, t)\vec{\mathbf{x}}_u q(\mathbf{x}, t)) + d\nabla^2 \cdot (u(\mathbf{x}, t)), \tag{1.20}$$

$$\frac{\partial}{\partial t} v(\mathbf{x}, t) = -c\nabla \cdot (v(\mathbf{x}, t)\vec{\mathbf{x}}_u p(\mathbf{x}, t)) + d\nabla^2 \cdot (v(\mathbf{x}, t)). \tag{1.21}$$

In this chapter we analyse an idealised case of the conspecific avoidance model described above. We consider two packs interacting in one spatial domain. Although this simplified version sacrifices some biological realism, but remains a toy model, it maintains almost the same qualitative features observed in higher dimension and with a greater number of packs.
Furthermore, we consider a non-dimensionalised form of the problem in a one dimensional space domain where the parameters and the variables are dimensionless quantities. Specifically, the steady state is governed by the following system:

$$\begin{cases} d\dfrac{\partial^2 u}{\partial x^2} - c\dfrac{\partial}{\partial x}(qu) = 0 & (1.22) \\ d\dfrac{\partial^2 v}{\partial x^2} + c\dfrac{\partial}{\partial x}(pv) = 0 & (1.23) \\ p = u(1 + mq) & (1.24) \\ q = v(1 + mp) & (1.25) \end{cases}$$

where u, v represent respectively the probability density function of pack U and V, p, q correspond to the scent mark densities of pack U and V and m is the sensitivity response of the scent mark to foreign scent marks.
Considering a spatial domain [0,1], we assume $u(0)$, $v(0)$ to be known. Furthermore, the curves u and v satisfy the following Neumann boundary con-

ditions:

$$d\frac{\partial u}{\partial x} - cqu = 0, \qquad d\frac{\partial v}{\partial x} - cpv = 0 \qquad \text{at } x = 0, 1 \tag{1.26}$$

and the integral condition

$$\int_0^1 u(x)dx = \int_0^1 v(x)dx = 1.$$

The value of m modifies the solution strategy for the system. Supposing $m \geq 0$, we can divide the problem in two cases: $m = 0$, where there isn't marking response, and $m > 0$.
Following the same approach used in Mechanistic Home Range Analysis, we consider a simplified version of the problem in which the boundary hold across the whole interval. Thus the system we solve becomes:

$$\begin{cases} d\dfrac{\partial u}{\partial x} - cqu = 0 \\ d\dfrac{\partial v}{\partial x} + cpv = 0 \\ p = u(1 + mq) \\ q = v(1 + mp). \end{cases} \tag{1.27}$$

When $m = 0$, since the expressions for p and q have been reduced to

$$p = u \qquad \text{and} \qquad q = v,$$

the system becomes:

$$\begin{cases} d\dfrac{\partial u}{\partial x} - cuv = 0 \\ d\dfrac{\partial v}{\partial x} + cuv = 0 \\ \int_0^1 u(x)dx = \int_0^1 v(x)dx = 1. \end{cases} \tag{1.28}$$

Thus, the analytical solutions of (1.28) are two logistic equations:

$$v(x) = \frac{2}{1 + e^{-\frac{2c}{d}(x-0.5)}} \qquad \text{and} \qquad u(x) = \frac{2}{1 + e^{\frac{2c}{d}(x-0.5)}}. \tag{1.29}$$

We notice that Eqs.(1.29) describe correctly the evolution of two packs' home ranges, assuming equal diffusive and advective responses to the environment. However, taking $c_u \neq c_v$ or $d_u \neq d_v$, the density equations u and v should

have different formulations, in particular the ratio c/d. On the other hand a numerical approach can estimate correct solutions in both cases, whether the coefficients are equal or different for the packs, because we can provide these parameters at the beginning of the code separately. Therefore, if c and d are unique for U and V, both the numerical and analytical approach reproduce an accurate estimation of the pack densities; otherwise only the numerical code can reflect the real spatial distribution. In the following figures we can see the two different cases:

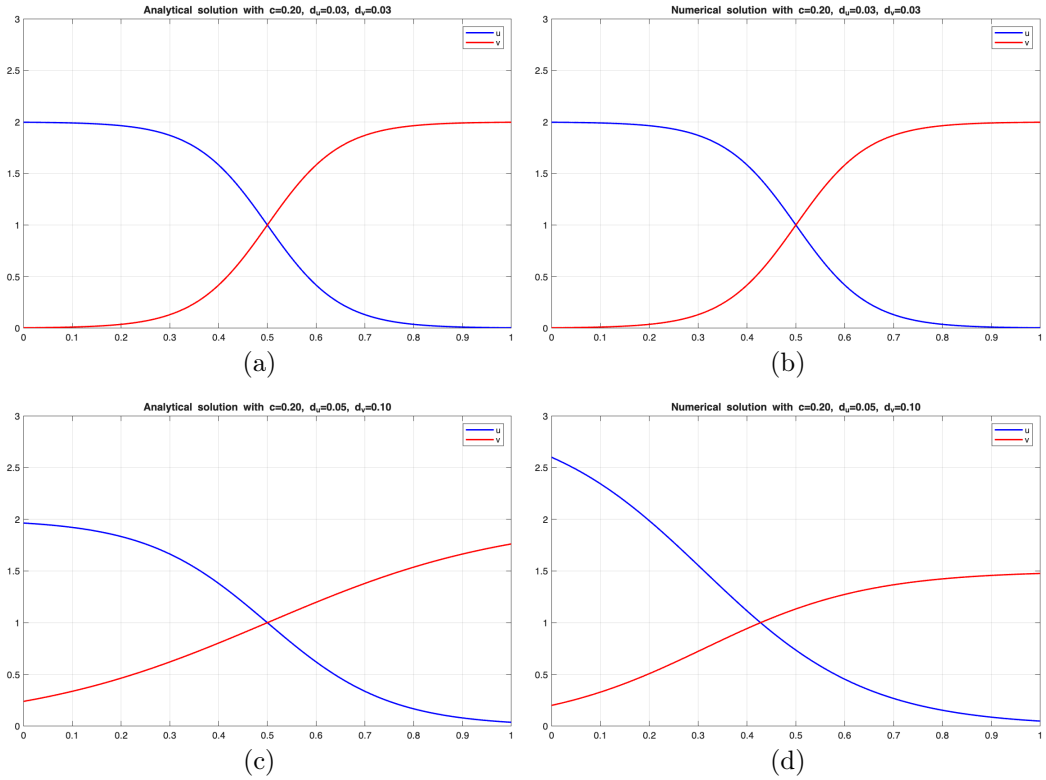

Figure 1.2: Case with m=0. (a) and (b) represent the analytical and numerical solutions when U and V have the same parameters c and d. The case in which $d_u \neq d_v$ is illustrated in panel (c)(analytical case) and (d)(numerical case).

We have considered for the spatial domain the interval $[0, 1]$, whose endpoints coincide with their dens, respectively, in 0 and 1 for U and V.
Let us now consider the case where the marking response m is positive. In this case, solving the system (1.27), we find an expression for p and one for q depending only on u, v and m:

$$p = \frac{u(1+mv)}{1-m^2uv}, \qquad q = \frac{v(1+mu)}{1-m^2uv}. \tag{1.30}$$

Substituting Eqs. (1.30) in (1.27) yields

$$\begin{cases} d\dfrac{\partial u}{\partial x} - c\dfrac{v(1+mu)}{1-m^2uv}u = 0 \\ d\dfrac{\partial v}{\partial x} + c\dfrac{u(1+mv)}{1-m^2uv}v = 0, \end{cases} \tag{1.31}$$

and solutions can be found analytically, for instance v has the following expression:

$$v(x) = \frac{1}{2m^2v(0)}\left(\sqrt{\left(e^{\frac{-cx}{dm}}(1-m^2u(0)v(0))\right)^2 + 4m^2v^2(0)} + \right. \tag{1.32}$$
$$\left. - e^{\frac{-cx}{dm}}(1-m^2v^2(0))\right)$$

and analogously for u.
Finally we need to impose the initial conditions $u(0)$, $v(0)$ to satisfy the integral constraint and using the same reasoning applied above, we compare only the case $m > 0$ when U and V have the same ratio $\frac{c}{d}$:

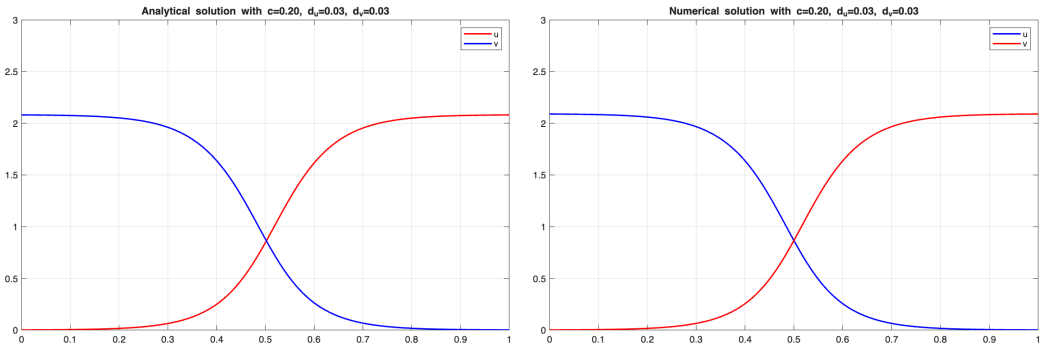

(a) (b)

Figure 1.3: m=0.48

1.2.2 Advection-Diffusion for passerines

The advection diffusion equation has also been useful in describing home ranges of flocks of long-tailed tits. This is different from wolves where their

movements are based on prey availability and the location of a den site. Unlike these predators, long-tailed tit home ranges have no clear central point, nor do they use aggression or scent marks to delineate their territory. Nevertheless both spatial dynamics could be analysed using a PDE framework. This was made possible by Potts and Lewis (2016), who generalised the existing PDE methodology developed for animals with clear den site and scent mark avoidance. They proposed a mechanistic home range analysis capable of studying home ranges built on different underlying rules rather than territorial marking or den-oriented patterns.
Long-tailed tits live in flocks and they exhibit avoidance responses toward conspecific flocks. This behaviour is inversely proportional to the size of the flocks and the relatedness between them: for smaller flocks the avoidance magnitude is greater than for the larger ones. Unlike wolves, these birds use avoidance and vocalising as a proxy for territoriality to prevent encounter with other flocks. Since they do not have a fixed nest, their movement patterns are influenced by other factors, such as landscape characteristics and cognitive processes. Specifically these animals exhibit a preference toward a woodland area, and they appear to possess a spatial memory, although not yet biologically proven, they avoid trees previously occupied by other flocks. Thus, to account for all these behavioural decisions, a mechanistic modelling approach is essential for analysing long tailed tits home ranges.
Long-tailed tits have been studied in Rivelin Valley, Sheffield, UK, from 1994 and for the 2011–2012 and 2018-2019 seasons, location data from six flocks were collected in the Fox Hagg woodland of the Rivelin Valley (Ellison et al., 2020). These flocks have more than 40 relocations taken over more than one observation period. It appears that the best approach to model their home ranges is to consider both avoidance with respect to other flocks and a tendency towards the centre of the woodland area. Incorporating this behaviour solely into the advection term c is more effective, also because studies have shown that adding it to the diffusion coefficient produces a poorer fit.
Let us consider the following system of advection-diffusion equations in a two dimensional space:

$$\frac{\partial u_i}{\partial t}(\mathbf{x},t) = D_i \nabla^2 u_i(\mathbf{x},t) - c_i \nabla \cdot [u_i \mathbf{A}_i(\mathbf{x},t)]. \tag{1.33}$$

Here we consider $\mathbf{x} = (x, y)$ and u_i as the flock densities, which are studied taking into account their relatedness to one another and for landscape characteristics, such as food availability. In Eq. (1.33) parameters D_i represent the diffusion term associated with foraging, while c_i is the advection coefficient, governed by the avoidance tendency and the woodland attraction. The

vectors $\mathbf{A}_i(\mathbf{x}, t)$ provide directions of movement patterns of each flock i.
In order to reduce the complexity of the system, we suppose that all flocks have the same diffusion and advection coefficients. Thus, we can rename them as $D_i = D$ and $c_i = c$. It is important to consider at least two behavioural components, which will define $\mathbf{A}_i$, with respect to long-tailed tits: the preference for woodland area and the interaction with conspecific flocks. Therefore, we consider an interaction zone (IZ) for each flock, an area where long-tailed tits remember past interactions with other flocks, and we define $k_i(\mathbf{x}, t)$ as the probability of a location $\mathbf{x}$ to be in the interaction zone. These dynamics give rise to the equation written below:

$$\frac{\partial k_i}{\partial t} = \rho u_i \sum_{i \neq j} u_j (1 - k_i) - \beta k_i u_i, \tag{1.34}$$

where ρ is the rate at which the IZ is reinforced when two flocks of long-tailed tits are at the same location and β is the decay rate of the IZ due to revisiting areas without encountering other flocks.
Tits consider a small area around that location when making movement decisions, and not the infinitesimally precise location. The most realistic approach is to assume this area corresponds to a disc B of radius δ centred in $\mathbf{x}$. Thus, we must consider an average on all $k_i(\mathbf{x}, t)$ over the disc. Mathematically, $\overline{k_i}(\mathbf{x}, t|\delta)$ has the following expression:

$$\overline{k_i}(\mathbf{x}, t|\delta) = \frac{1}{\pi \delta^2} \int_{B_\delta(\mathbf{x})} k_i(\mathbf{x}, t) d\mathbf{x}. \tag{1.35}$$

Moreover we must consider a vector field in $\mathbf{A}_i$ that describes the attraction toward woodland, defined $\mathbf{v}_M$.
This leads to a definition of the total advection vector:

$$\mathbf{A}_{i,M} = -c_1 \nabla \overline{k_i} + c_2 \mathbf{v}_M, \tag{1.36}$$

where c_1 and c_2 represent the magnitude of advection away from the IZ and toward woodland area. The index M denotes the specific model used to analyse home ranges and for most of the studies the best model is the one that assumes birds prefer to move toward the woodland, if they are outside, and if they are already in it, toward the centre of the woodland area.
Furthermore, to maintain biological realism, we consider two additional equations associated with Eqs. (1.33)-(1.36): Eq (1.37) guarantees that each u_i is a probability density function by imposing the integral to be 1 over the domain Ω; Eq (1.38) reflects the assumption of a constant number of long tailed tits in the study area by taking the zero flux, or Neumann, boundary

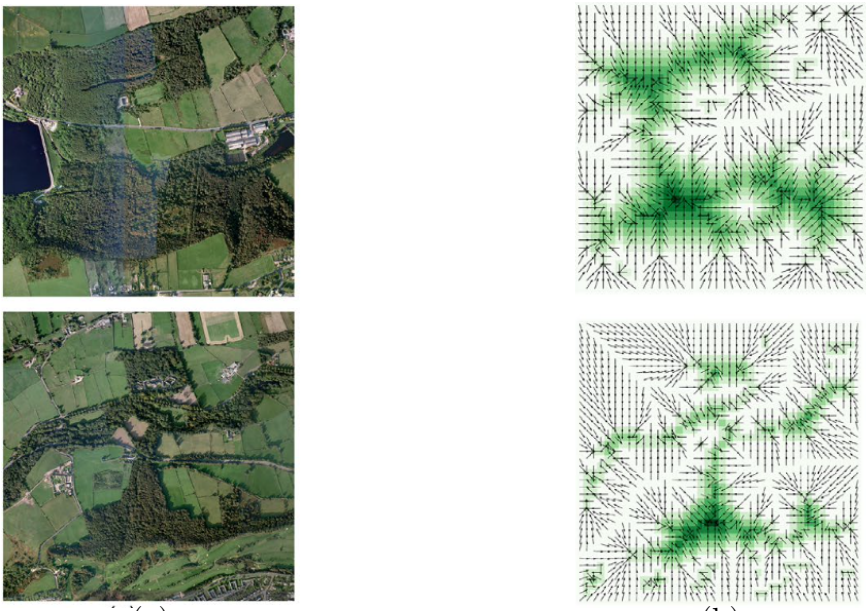

(a) (b)

Figure 1.4: Panel (a) is the photograph of woodland for the Fox Hagg (top) and Black Brook (bottom). Panel (b) represents the vector field $\mathbf{v}_M$ for the model corresponding to the woodland images on (a), respectively.

condition:

$$\int_{\Omega} u_i \, d\mathbf{x} = 1, \tag{1.37}$$

$$|\mathbf{n}_x \cdot (D\nabla u_i - cu_i\mathbf{A}_i)|_{x\in\partial\Omega} = 0 \tag{1.38}$$

where $\mathbf{n}_x$ represents a vector normal to the boundary of the domain $\partial\Omega$ at $\mathbf{x}$.

By nondimensionalising the system of Eqs. (1.33)-(1.38) and studying its steady state solution has been obtained the utilisation distribution of long tailed tits during the non breeding season in the Rivelin Valley. The model provides home ranges of six observed flocks. We can notice in the following figures that the clustering of six flocks is present in both woodland images, panels (a) and (c), and model simulations, panels (b) and (d); furthermore, the models provide an accurate approximation of the actual home ranges.

Analogously to the mechanistic home range models developed for long tailed tits, Moorcroft and Lewis analysed two dimensional home range models for coyotes packs. They introduced different mechanistic methods, taking into account various factors, such as prey availability, steepness of the terrain and conspecific avoidance. Depending on the factor that most influenced the

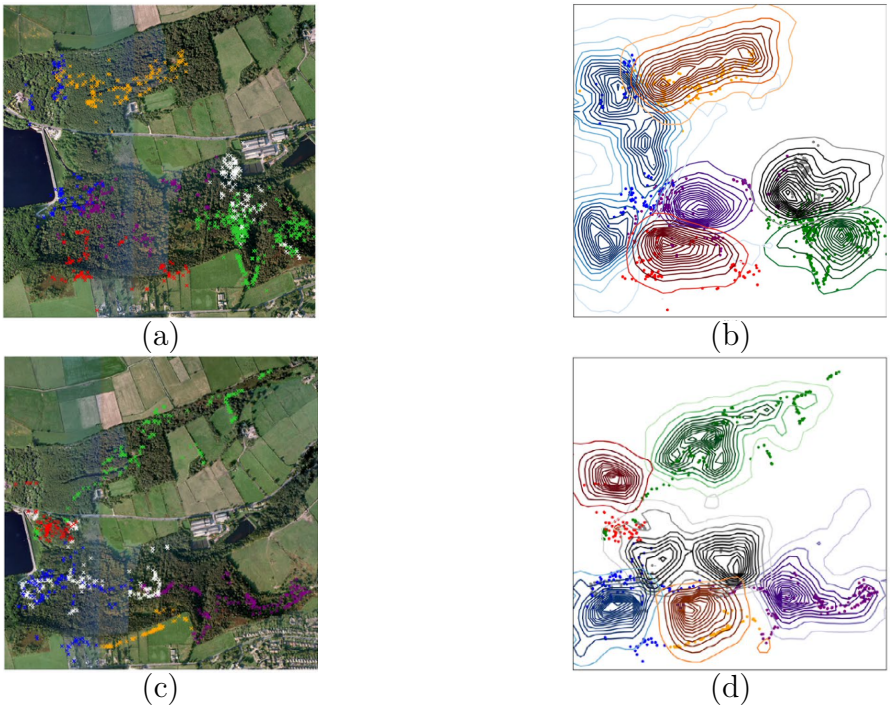

Figure 1.5: Panel (a) and (c) show the real locations of six flocks in Fox Hagg woodlands, Rivelin Valley, during non breeding season of 2011-2012 and 2018-2019, respectively; panel (b) and (d) provide the utilisation distributions in a two dimensional space domain by fitting the steady state solution of Eqs (1.33)-(1.38) to data from 2011-2012 and 2018-2019, respectively.

animal's movements, one model predicted the spatial distribution of coyotes movements more accurately than another. We report here two different models: in the first image, coyotes present sensitivity to foreign scent mark, exhibiting an avoidance response to conspecifics (Fig. 1.6, panel (a)); in the second it is presented a model in which conspecific avoidance and steepness terrain avoidance have the main responsibility for coyotes movement patterns.
The advection diffusion equations for the koala home range are developed by integrating different mechanistic approaches from the previously discussed models for passerines and wolves. Specifically, we implement a conspecific avoidance model to describe the probability density function of two koalas, where avoidance is interpreted as a social response, similar to the wolves model. Furthermore, long-tailed tits framework demonstrates that an advection-diffusion system could be accurate to describe a species' home range even if it does not have a clear central point, such as a den or a nest. Since koalas do not exhibit movements biased toward a fixed central point,

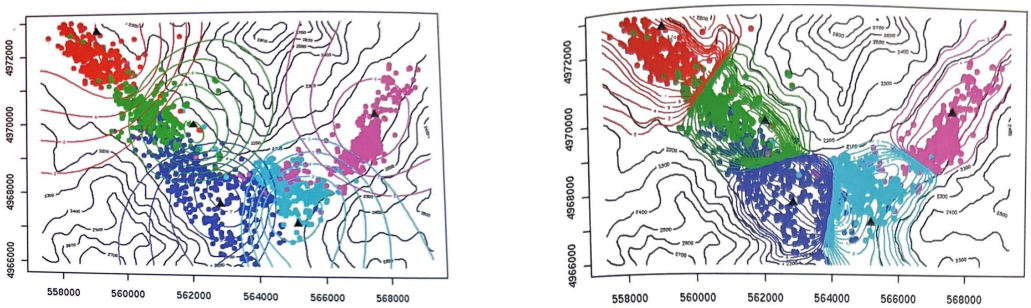

(a) (b)

Figure 1.6: (a) Contour lines showing fit of the conspecific avoidance (CA) (panel (a)) and the steepness terrain avoidance plus conspecific avoidance (STA+CA) (panel (b)) home range model to relocation data (•) for five packs of coyotes in Lamar Valley. Gray contour lines show topography relief in meters. Colored contour lines show the probability density function $u^{(i)}(x, y)$ for each pack (i=0...5). The home range centers for each pack are shown (▲).

this comparison confirms the validity of using a modified advection-diffusion model to describe their spatial distribution and home range patterns.

Chapter 2

Numerical solutions for the koalas' home range

In this chapter we will discuss the numerical steady state solutions of the advection-diffusion system that describes the one-dimensional home range of two koalas, respectively u and v, short distances apart from each other so that an encounter between them is possible.
As observed in the previous chapter, the non dimensionalisation of the advection-diffusion system is an essential step because it reduces the complexity of the problem and allows for a generalised approach, independently from the specific biological behaviour of the species. Here, our goal is to apply the same methodology to investigate the interaction between two koalas living in the same domain and consequently model how their home ranges modify and evolve in response to one another.

2.1 Non-Dimensionalisation for Koala and other species

We take into consideration the general form of the advection-diffusion equation and adapt it to describe and predict the home ranges of koalas, starting from the following modified version of the system presented in Mechanistic Home Range Analysis (Moorcroft and Lewis, 2006).

$$\frac{\partial u}{\partial t} = d\nabla^2 u - c\nabla \cdot [u\vec{\mathbf{x}}_u q], \tag{2.1}$$

$$\frac{\partial v}{\partial t} = d\nabla^2 v - c\nabla \cdot [v\vec{\mathbf{x}}_v p]. \tag{2.2}$$

In our case, $u(\mathbf{x},t)$ and $v(\mathbf{x},t)$ represent the densities of two koalas U and V respectively. The $\vec{\mathbf{x}}_u$ and $\vec{\mathbf{x}}_v$ are unit vectors pointing toward the center of the home range of koala U and V respectively, c is the advection coefficient and d is the diffusion coefficient. Similarly to the case of other species, we introduce a mechanism for contact inhibition, through scent.
If $p(\mathbf{x},t)$ and $q(\mathbf{x},t)$ represent the density of the scent marks of koala U and V, they follow the equations given by:

$$\frac{\partial p}{\partial t}(\mathbf{x},t) = Nu(\mathbf{x},t)(l + mq(\mathbf{x},t)) - \mu p(\mathbf{x},t), \tag{2.3}$$

$$\frac{\partial q}{\partial t}(\mathbf{x},t) = Nv(\mathbf{x},t)(l + mp(\mathbf{x},t)) - \mu q(\mathbf{x},t) \tag{2.4}$$

where N is the number of animals per pack, for us $N = 1$, as koalas are solitary; μ is the rate of scent mark decay; l is the rate at which a koala provides scent marks in absence of foreign scent marks and m denotes the sensitivity of the marking response to foreign scent marks.
It can be useful to nondimensionalise Eqs. (2.1)-(2.4) introducing the following variables in line with the procedure illustrated by Moorcroft and Lewis (2006).

$$\begin{aligned}
&x^* = \frac{x}{L}, && y^* = \frac{y}{L}, && t^* = t\mu, && u^* = L^2 u,\\
&v^* = L^2 v, && p^* = \frac{L^2\mu p}{Nl}, && q^* = \frac{L^2\mu q}{Nl}, &&\\
&d^* = \frac{d}{\mu L^2}, && c^* = \frac{clN}{\mu^2 L^3}, && m^* = \frac{mN}{\mu L^2} &&
\end{aligned} \tag{2.5}$$

where L is a characteristic length scale that is related to the area A ($A = L^2$) of the spatial domain over which data have been collected and the system of equations is solved.
The distance travelled by one koala daily can vary depending on the area of the study. For instance, the average distance travelled in one day by male and female koalas, in the area around Ballarat, in the State of Victoria, is 207 and 70 meters respectively (Hull, 1985). Considering the following values of parameters, which align with typical data in the surveys, we have:

$$L \approx 100\text{m}, \quad \mu = 1 \text{ day}^{-1}, \quad N = 1, \quad l = 1 \text{ day}^{-1} \quad \text{and} \quad p, q = 1 \text{ m}^{-1}.$$

Dropping the asterisks in (2.5), for simplicity in writing, and substituting in Eqs. (2.3)-(2.4), the non-dimensionalised system becomes:

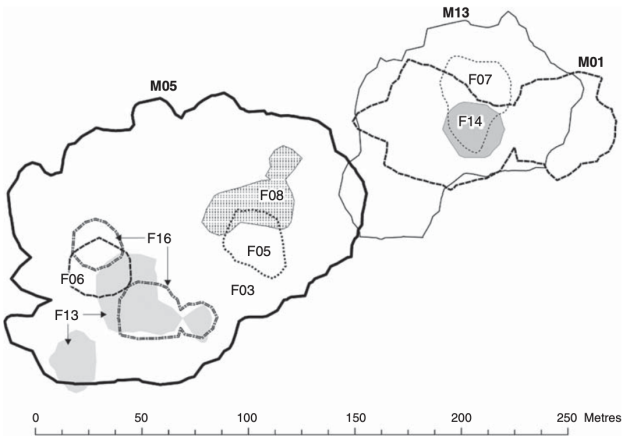

Figure 2.1: An example of the spatial distribution of interacting male and female koalas. Total ranges are shown for three males, and core use areas shown for eight females. Male M05 interacted for a total duration of >30 min with each of the six females with core areas inside his range. M01 and M13 interacted for >30 min with each other and with F07 and F14. Cape Otway, Victoria, 2015 (Watchorn and Whisson, 2019)

$$\begin{cases} \dfrac{\partial u}{\partial t} = d\nabla^2 u - c\nabla \cdot [u\vec{\mathbf{x}}_u q] \\ \dfrac{\partial v}{\partial t} = d\nabla^2 v - c\nabla \cdot [v\vec{\mathbf{x}}_v p] \\ \dfrac{\partial p}{\partial t}(\mathbf{x},t) = u(\mathbf{x},t)(1+mq(\mathbf{x},t)) - p(\mathbf{x},t) \\ \dfrac{\partial q}{\partial t}(\mathbf{x},t) = v(\mathbf{x},t)(1+mp(\mathbf{x},t)) - q(\mathbf{x},t) \end{cases} \tag{2.6}$$

Generally speaking, this is a system of nonlinear PDEs defined in an n-dimensional space domain, where n corresponds to the dimension of the vector $\mathbf{x}$. The focus of the present thesis is to concentrate on the nondimensionalised case and provide different ways of interpreting and solving the problem. As we will see, each way carries a very interesting and new set of insights into the understanding of koala's home ranges.

2.2 Definition of the problem

In this section we look at the mathematical settings that allow us to find the steady-state solutions of the system (2.6) in a one-dimensional space domain

[0, 1]. We firstly set to zero the partial derivative with respect to time, so that the problem we are solving has the following formulation:

$$\begin{cases} d\dfrac{\partial^2 u}{\partial x^2} - c\dfrac{\partial}{\partial x}(qu) = 0 & (2.7) \\ d\dfrac{\partial^2 v}{\partial x^2} - c\dfrac{\partial}{\partial x}(pv) = 0 & (2.8) \\ p = u(1+mq) & (2.9) \\ q = v(1+mp). & (2.10) \end{cases}$$

Furthermore, boundary conditions are given at $x = 0, 1$ and are zero-flux (or von Neumann) conditions, implying that both U and V cannot leave the domain.
As we will see, this choice influences the character of any solutions. Formally this requirement translates into the following system:

$$\begin{cases} d\dfrac{\partial u}{\partial x} - cqu = 0 \quad \text{at } x = 0, 1, & (2.11) \\ d\dfrac{\partial v}{\partial x} - cpv = 0 \quad \text{at } x = 0, 1. & (2.12) \end{cases}$$

The functions u and v are mathematically represented as two probability density functions, and therefore they have to satisfy the normalisation constraint:

$$\int_0^1 u(x)dx = \int_0^1 v(x)dx = 1. \tag{2.13}$$

To solve the system of Eqs. (2.7)-(2.10) we also need to choose constraints at the edge of the interval for u and v in the domain. Let us take into account two different cases: first we assume two koalas near the same tree, where one individual has somehow more "dominance" over the other and tends to occupy that "area" more frequently. As for the case of other species, this can be translated into the condition $u(0) = 1$ and $v(0) = 2$. Secondly we analyse the case in which U and V are at the opposite boundary of the domain, and still V has an overall stronger presence, therefore $u(0) = 1$ and $v(1) = 2$. With these conditions, we solve the equations (2.7)-(2.10) numerically, using MATLAB software. Details of the algorithm we use are in Appendix B. Note that conditions (2.11)-(2.13) are also imposed, and we verify that they are satisfied in all the solutions presented in the following. The figures in the next sections illustrate the evolution of the curves with the progression of parameters, both the marking response to foreign scent marks, m, and the

diffusive coefficient d. Since each coefficient c in the system is associated with d, we choose to keep c invariant across all plots; the ratio c/d changes between different figures. We also maintain over the figures the same parameter m for each pair of curves u and v.

2.3 Koalas close to the same tree

In this case, we consider two koalas located on the same tree or on trees very close in relation to the spatial scale of the domain, both exhibiting a tendency to move in the same direction, toward the opposite endpoint of the interval (at x=1). In other words, they are moving away from the origin. As said, we assume $u(0) = 1$ and $v(0) = 2$; the functions u and v represent the probability density functions of the spatial distribution of U and V, respectively, in the domain $[0, 1]$.

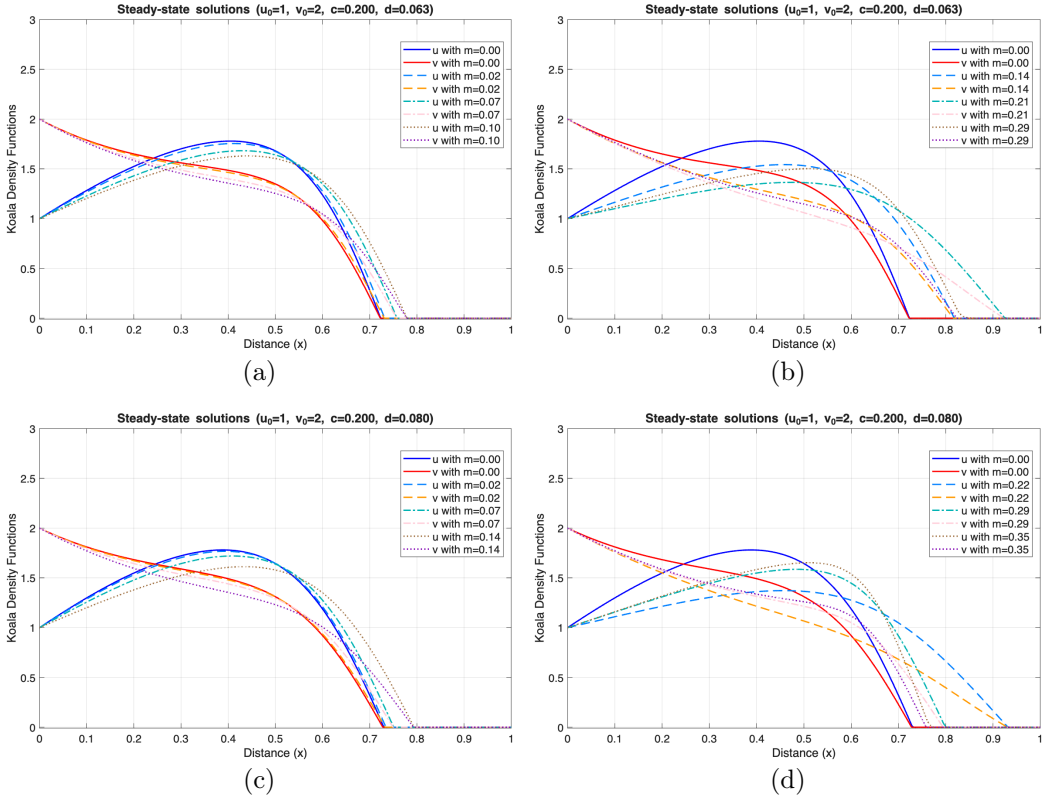

Figure 2.2: Comparison between panels with different parameters: panels a) and b) show the steady-state solution for $d = 0.63$ with varying m from 0 to 0.29; panels c) and d) illustrate the steady-state solution for $d = 0.80$ and varying m from 0 to 0.35.

Initially, we impose a fixed ratio c/d for all pairs of curves u and v in each panel. This ratio is kept below 1 in all cases except for panels c) and d) in Fig. 2.4. There, we explore the cases where the attraction toward the end of the domain is greater than the diffusivity. This can represent the case where another tree is present at x=1.
Each panel illustrates two families of curves that describe the probability density function u and v for koala U and V, respectively, assuming different parameters. In Fig. 2.2, specifically when m and d are small (for example panel (a)), most of the area under the curve is concentrated in the first half of the interval, and this suggests that there are areas where co-occurrence between the two koalas is more likely when they are close to the initial tree, set at x=0. This aptitude to interact decreases rapidly with the distance from the tree.

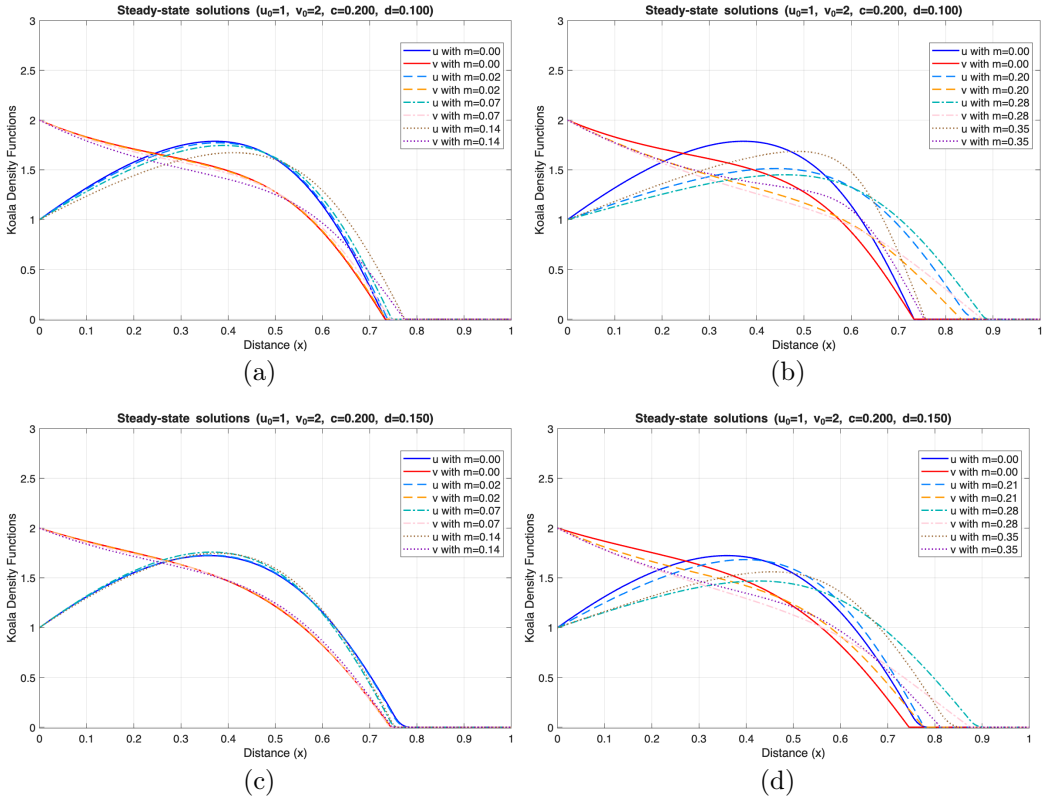

Figure 2.3: Comparison between solutions with different parameters: panels a) and b) show the steady-state solution for $d = 0.1$ with varying m from 0 to 0.35; panels c) and d) illustrate the steady-state solution for $d = 0.15$ and varying m from 0 to 0.35.

Results in Fig. 2.2 suggest that a larger marking response has a greater

impact on the spatial distribution of the koalas than an increase of d. This is quite interesting and represents a new result. For instance, the changes of profiles in u and v with the increase in scent response m from panel a) to panel b) are more evident than the plots in panel c). We can see that in b) the functions are flattening, their decline toward x-axis is more gentle and that the regions of higher overlap shift away from the initial location at x=0. If sensitivity to the foreign scent mark is high, koalas are driven to move away from each other; the model suggests that the repulsion between them leads to a shift of the peak of overlap from the initial tree further to the right.

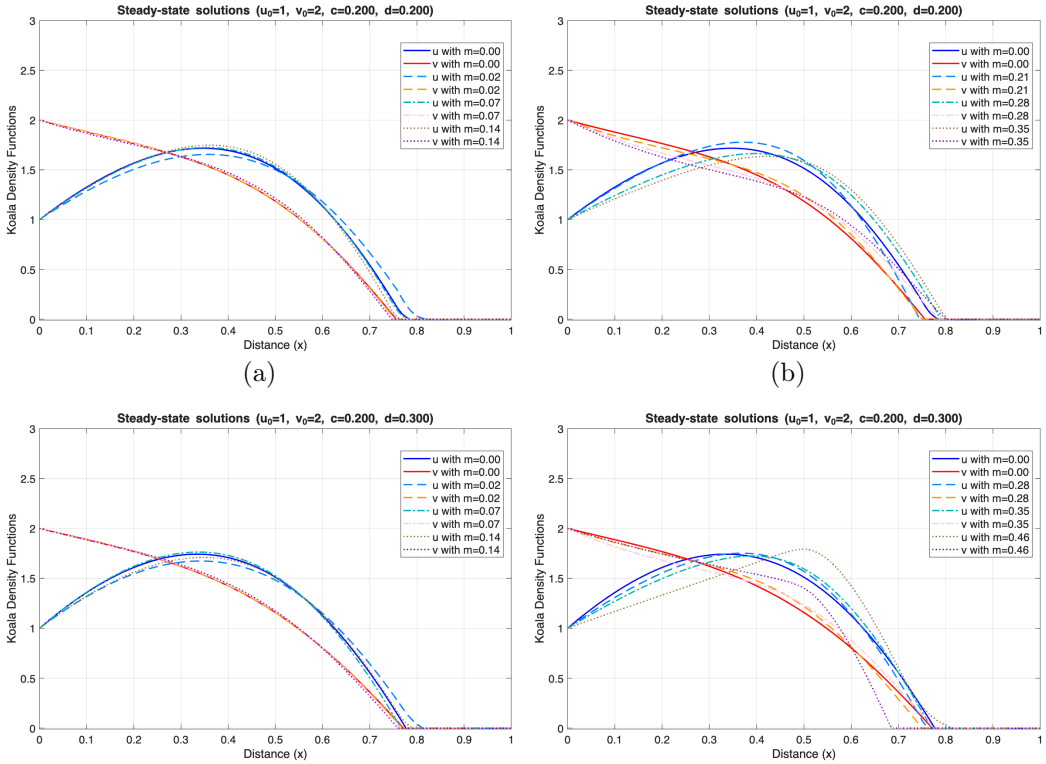

Figure 2.4: Comparison between solutions with different parameters: panels a) and b) show the steady-state solution for $d = 0.2$ with varying m from 0 to 0.35; panels c) and d) illustrate the steady-state solution for $d = 0.3$ and varying m from 0 to 0.35.

A cross-analysis of Figs. 2.2-2.4 reveals that, increasing the diffusive coefficient d, leads to a minor effect from increasing m. A koala becomes less sensitive to other scent marks when it is more motile and has a larger associated diffusive coefficient. Therefore, a higher value of m is required to notice

a significant deviation from the case $m = 0$. Comparing panels across these figures, it is notable that, with the same sensitivity to marking response (or sufficiently close to), the solutions progressively return to the base case with no scent sensitivity.
If koalas exhibit limited motility, the model suggests that scent marks act as a primary inhibitor of social interaction, and m influences the koalas' dynamics more than in the scenario of a higher diffusion component.
Note also that solutions to this problem, which requires an area under the curves to be non negative, can be sometimes not physically and biologically relevant, and assume a negative profile after intersecting the x-axis.
The same behaviour occurs for the analytical solutions, as we will show shortly. For this reason we decide to truncate the solution at the intersection between the curve and the x-axis. This approach is frequently used in similar cases within the field of mathematical biology to guarantee ecological consistency of the model, in particular when a strong value of repulsion is present. In addition, the simultaneous imposition of the zero-flux boundary and the fixed point at boundary for u and v can be seen as adding more reality to the model. For example, this mathematical framework allows us to interpret the boundaries of the interval as physical obstructions, preventing the animals from escaping the domain, thus representing anthropogenic barriers, such as roads and fences, that koalas sometimes encounter in their home ranges (Lassau et al., 2008). Similarly, koala habitats are often disrupted by bushfires, that result in great limitations to koalas' movement (Matthews et al., 2016).
Let us now consider a different ratio c/d between pairs of functions u, v. Following the same approach used above, we keep the advective parameter c fixed at 0.2, and vary the parameter d: Fig. 2.5 reveals some differences with respect to those analysed previously, but it is noteworthy that the resulting curves consistently follow the trends discussed above, with d and m providing opposing forces to koalas behaviours. Note also that the extension of the domain area where encounters are possible is increasing with m at fixed c/d.

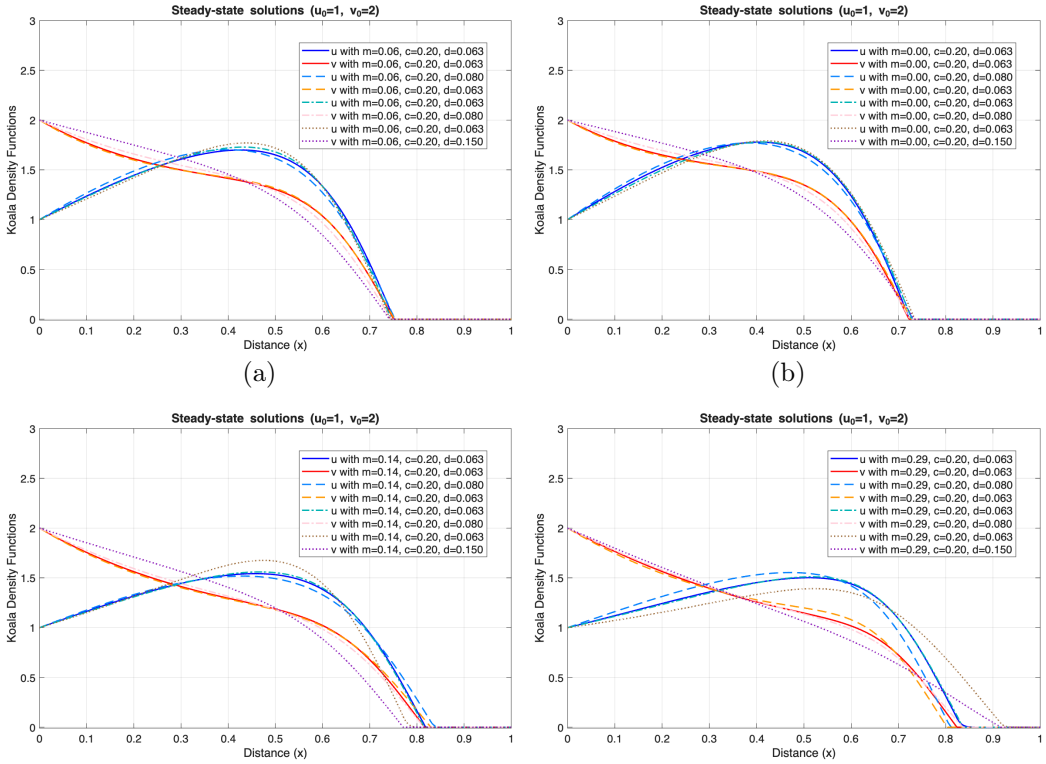

Figure 2.5: Comparison between solutions with different parameters. Across the panels, m ranges from 0 to 0.29, while c is kept constant at 0.2. The variations observed are regulated by d that varies from 0.063 to 0.15 in each panel.

2.4 Koalas on different trees

Let us now consider two koalas at the opposite endpoints of the domain: koala U is located at x=0, with $u(0) = 1$, and, choosing $v(1) = 2$, koala V stays at x=1. Integrating the equations with these conditions, we observe different profiles for koalas' spatial distributions. Notably, the family of curves associated with koala V exhibit an evident change in curvature with the variation of parameters. Also, the geometry of the problem is such that a pronounced maximum is not present as in previous figures, and higher local values for u and v shift toward the end of the domain. In this scenario the area near the second tree at x=1 seems to be the one where overlap is more likely to occur. Notably, a high magnitude of m emerges as a sort of "defence" mechanism by the koala V for its initial location. Territoriality is evidenced by the increasing character of v, with a pronounced maximum close to x=1. It

is important to remind that the direction of $\vec{\mathbf{v}}$ is towards x=1, so koala V has a strong propensity to be extremely close to the right endpoint of the domain.
While scent marks still have a significant impact on koalas' dynamics, they shape the probability density functions differently. For example, Fig. 2.6 illustrates that, increasing the magnitude of m, maxima begin to emerge, however they remain less distinctive than those previously discussed. Another difference concerns the sign of the functions: here curves remain positive across almost the entire domain because the initial distances between the two koalas already limit the possibility to share space and there is relatively large space in the domain when the inhibition due to scent marking is not perceived, due to the large distance between koalas.

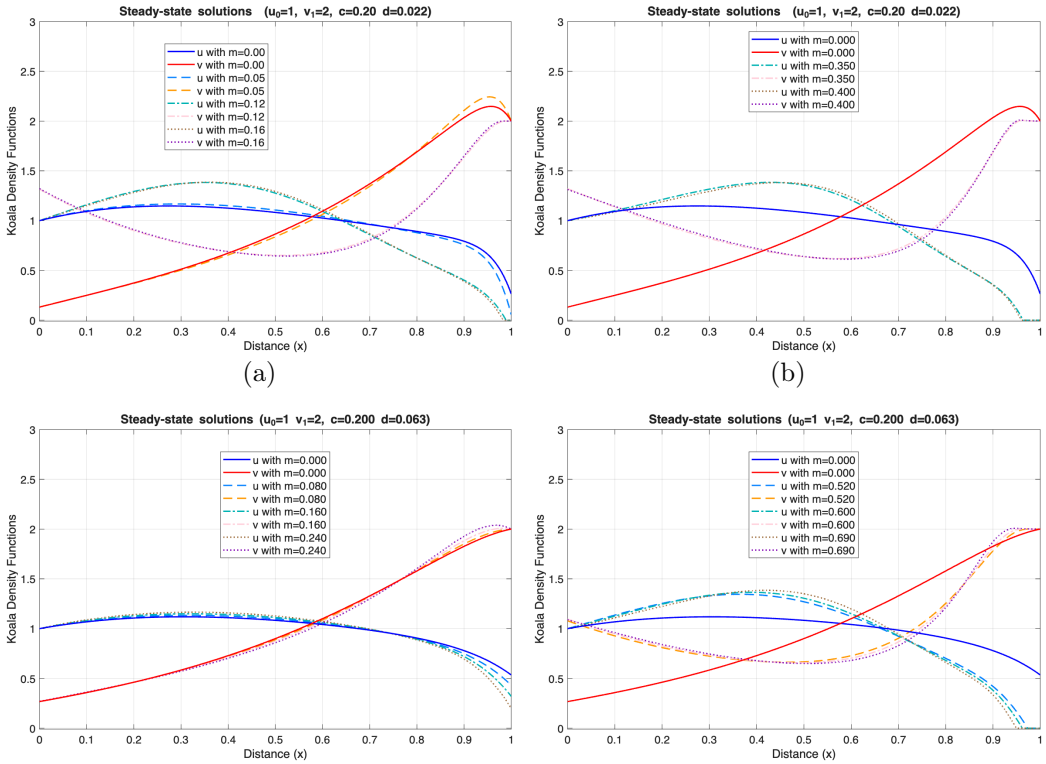

Figure 2.6: Comparison between solutions with different parameters: panels a) and b) show the steady-state solution for $d = 0.022$ with varying m from 0 to 0.4; panels c) and d) illustrate the steady-state solution for $d = 0.063$ and varying m from 0 to 0.69.

Increasing the value of d three times attenuates the effect of sensitivity to scent marks and, consequently, substantially higher values of m are required

to generate similar curves (Fig. 2.6). Furthermore, the presence of higher motility in koalas, corresponding to an increase in d, leads to a reduction of the maxima at the end of the domain (panel d) of Fig. 2.6 for koala V and allows for smaller spatial overlap for U, which is able to move away from the region occupied by V.

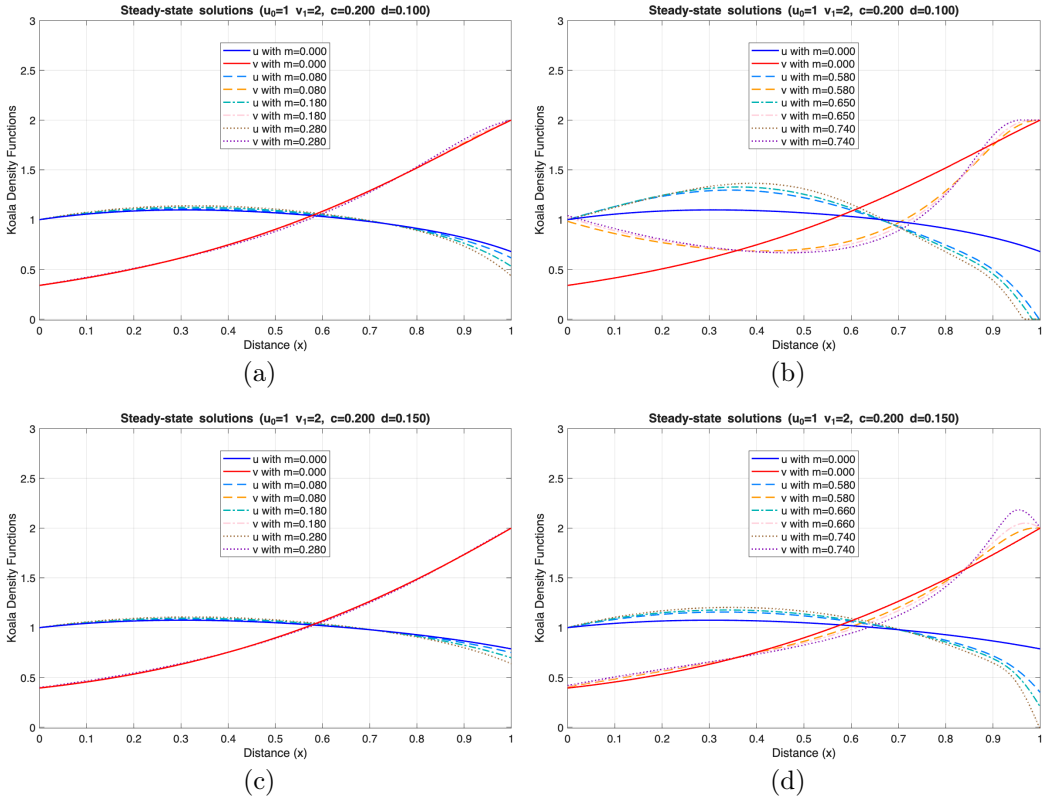

Figure 2.7: Comparison between solutions with different parameters: panels a) and b) show the steady-state solution for $d = 0.1$ with varying m from 0 to 0.74; panels c) and d) illustrate the steady-state solution for $d = 0.15$ and varying m from 0 to 0.74.

By increasing d even further, given the same value of m, the density functions almost converge toward each other,their shapes tending toward a polynomial or exponential shape as d grows. For m small enough (panels a) and c), Fig. 2.7) it is evident that the regions of higher overlap remain close to the centre of the domain.
In both Figs. 2.7-2.8, the curves follow a trend similar to that illustrated in Fig. 2.6. However, while in Fig. 2.7 panel b), a change in the sign of the curvatures occurs, as in previous figures, this variation is not yet observed in Fig. 2.7 (panel d) and Fig. 2.8 (panels b and d). This suggests that koala

motility plays an essential role in determining whether the second koala is capable of moving away from the neighbourhood of the initial condition. It is interesting to observe how motility, given the same m, impacts how closely the curves resemble the monotonic case. This results in a highly nonlinear effect where typical factors such as the shift in concavity, the presence of a maximum near the initial position of V and the positivity of u throughout the entire interval have significant variations depending on the value of d.

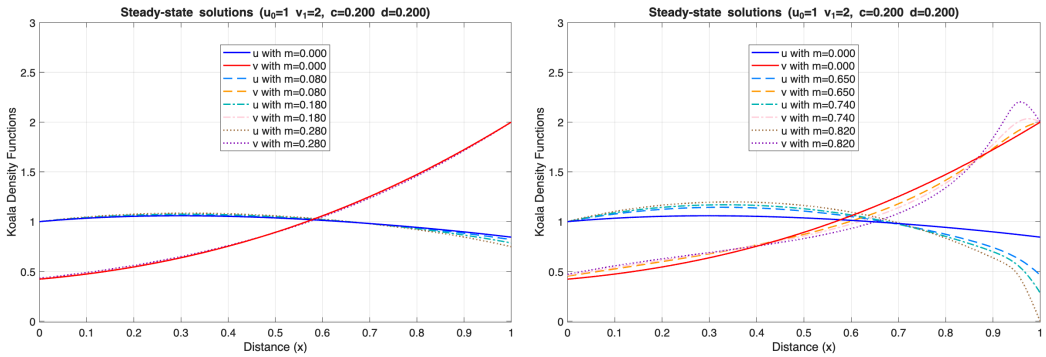

(a)

(b)

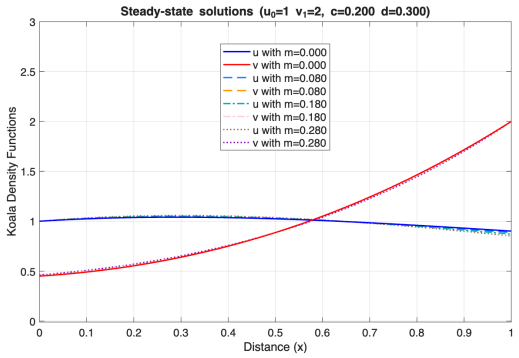

(c)

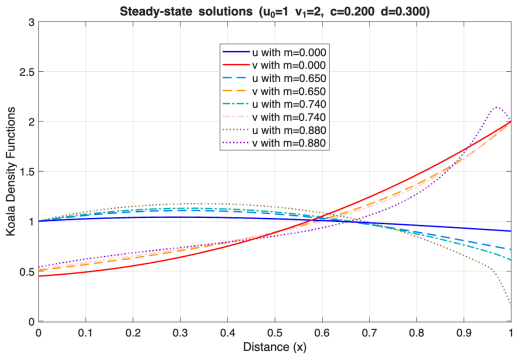

(d)

Figure 2.8: Comparison between solutions with different parameters: panels a) and b) show the steady-state solution for $d = 0.2$ with varying m from 0 to 0.82; panels c) and d) illustrate the steady-state solution for $d = 0.2$ and varying m from 0 to 0.88.

One point to strengthen is that this model does not account for koalas actual mass and U and V are treated as points that can overlap and compenetrate. In other words, koalas are able to "go through" each other, as if they were "ghosts" without a material extension. This is one of the limitations of this approach.

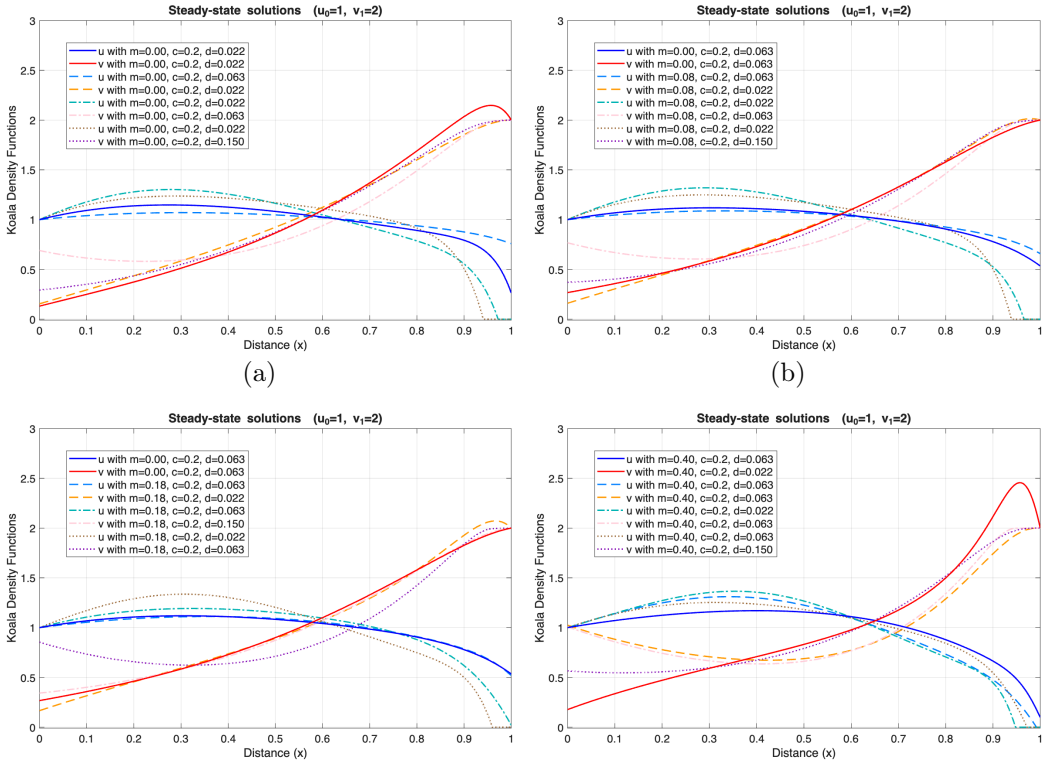

Figure 2.9: Comparison between solutions with different parameters. Across the panels, m ranges from 0 to 0.49, while c is kept constant at 0.2. The variations observed are regulated by d which varies from 0.063 to 0.15 in each panel.

Finally, it is interesting to analyse the case where some pairs of functions $u,\ v$ have different ratio $\frac{c}{d}$, where we can, similarly to the previous case, consider c fixed at 0.2 and vary the diffusivity value. The Fig. 2.9 reveals some differences with respect to those analysed previously, but it is noteworthy that the resulting curves consistently follow the trends discussed above. Again, the effect of $m,\ c$ and d is nonlinear.

2.4.1 Conclusion

The analysis of two paradigmatic cases shows the ability of this model to provide interesting findings in a simplified home range scenario.
Such results could have important consequences for the repopulation of koalas and social interaction dynamics. In both cases discussed above, it is notable that interactions with conspecifics are rare because there is a high component

of inhibition due to repulsion toward foreign scent marks. As illustrated in the previous figures, it seems the interactions occur near a tree and they are generally rarer if two koalas are located close to two distinct trees.
Very interestingly, our results appear consistent with the data recorded recently at Cape Otway, Victoria (Watchorn, 2025), where young male koalas were observed interacting without fighting. They exhibit "affiliative" behaviours that include grooming, playing and vocalising to each other in soft calls. This observation is very rare but it seems to be a consequence of the overabundance of koalas in particular areas, such as the habitat where these interactions have been recorded. The fact that the koalas observed were young males, between 3 and 5 years old, could explain this behaviour. At young age koalas have not yet developed the strong marking response to scent marks characteristic of adults and they usually exhibit higher motility. Thus, according to our model, by assuming a large d and a sufficiently small m, it follows that young koalas have regions of higher overlap with each other, and this could be a conclusion that persists in more realistic settings. The result provided by our model can be generalised to two-dimensional habitats and can provide qualitative indications about a repopulation, culling and relocation. In fact, these equations can allow for evaluation of socially structured koala populations based on the position of trees, type of trees, age structure of the population and individuals characteristics.

Chapter 3

Analytical steady-state solution and numerical solutions of the PDE system

In this chapter, we will first discuss the analytical steady-state solutions of the advection-diffusion system that describes the one-dimensional home range of two koalas, respectively U and V, located at short distances from each other so that an encounter between them is possible. We concentrate on the simplest case, i.e. when m, the sensitivity of the marking response to foreign scent marks, is zero. Even in this case, an analytical solution is still very complex and it is not feasible to obtain a readable, compelling closed form for $m \neq 0$.
Afterwards, we illustrate the numerical solutions for the nonlinear PDEs system (3.18) to investigate the evolution over time t and the approach to a solution alike to a steady-state in the ODE case. It is also worthwhile to compare these results with the numerical steady-state solutions of the ODEs system obtained in the previous chapter, knowing that a one-to-one correspondence between these systems does not exist. This is because we are considering two nonlinear systems; thus some effects are observable only in the ODEs and others are unique for the PDEs. Note also that we focus on a version of the PDEs system where only Neumann boundary conditions are satisfied: enforcing the same conditions as the ODEs in the previous chapter is not possible.

3.1 Analytical solutions in the case of zero sensitivity to foreign scent marks

Recalling the generic equation in the previous chapter, if $m = 0$, Eqs. (2.9) and (2.10) for the scents reduce to $p = u$ and $q = v$, leading to the following:

$$d\frac{\partial^2 u}{\partial x^2} - c\frac{\partial}{\partial x}(vu) = 0, \tag{3.1}$$

$$d\frac{\partial^2 v}{\partial x^2} - c\frac{\partial}{\partial x}(uv) = 0, \tag{3.2}$$

with no flux boundary conditions at $x = 0, 1$:

$$d\frac{\partial u}{\partial x} - cvu = 0, \tag{3.3}$$

$$d\frac{\partial v}{\partial x} - cuv = 0 \tag{3.4}$$

Let us consider a nontrivial solution where $u(x) \neq v(x)$. Integrating the equations (3.1) and (3.2) with respect to x:

$$d\frac{\partial u}{\partial x} - cvu = k_1, \tag{3.5}$$

$$d\frac{\partial v}{\partial x} - cuv = k_2, \tag{3.6}$$

we can subtract one equation from the other and obtain:

$$d\frac{\partial(u-v)}{\partial x} = k_1 - k_2 \Longrightarrow u - v = \frac{(k_1 - k_2)}{d}x + k_3.$$

Calling $k_4 := \frac{(k_1 - k2)}{d}$, the new expression for u and v are:

$$u(x) = v(x) + k_4 x + k_3 \tag{3.7}$$

and

$$v(x) = u(x) - k_4 x - k_3, \tag{3.8}$$

showing that the solutions we will consider differ only for a linear formation. Thus, substituting these expressions for u and v just found, respectively in Eqs. (3.5) and (3.6), resultant expressions give rise to two Riccati equations, as shown below:

$$u' - \frac{c}{d}u^2 + \frac{c}{d}(k_4 x + k_3)u = \frac{k_1}{d}, \tag{3.9}$$

$$v' - \frac{c}{d}v^2 - \frac{c}{d}(k_4 x + k_3)v = \frac{k_2}{d} \tag{3.10}$$

where, given that the domain is one dimensional and solutions are independent of time, we have substituted partial derivatives with ordinary ones.
It is worthwhile to emphasise that we are now considering the most general analytical solutions to the equations describing home ranges. As such, we will investigate cases where all the parameters are free to take any value. This is goes beyond the biological reality, because not all solutions we find will correspond to cases that occur in the wild. We choose to explore the most general case because the equations (3.5)-(3.6) have not been yet investigated thoroughly in the available literature.
Let us consider $u(x)$ first. For equation (3.9) the general solution is given by the sum of a particular solution, called u_p, and another function u_1.
The first thing is to find a good particular solution. Starting from polynomial functions, we can have three different cases that could give us a particular solution, conditioning to some parameters value.
If we consider a constant particular solution $u_p = \alpha$, then

$$\frac{c}{d}(k_4 x + k_3)\alpha = \frac{c}{d}\alpha^2 + \frac{k_1}{d}$$

and

$$\begin{cases} \dfrac{c}{d}\ k_4\alpha = 0 \\ c\alpha^2 - ck_3\alpha + k_1 = 0. \end{cases}$$

Thus we have two options:

$$\alpha = 0 \qquad \text{and} \qquad k_1 = 0,$$

or

$$k_4 = 0 \Longrightarrow k_1 = k_2 \qquad \text{and} \qquad \alpha = \frac{ck_3 \pm \sqrt{c^2k_3^2 - 4ck_1}}{2c}.$$

Let us examine a linear particular solution $u_p = \alpha x + \beta$, imposing it in Eq. (3.9) and obtain $\alpha + \dfrac{c}{d}(k_4 x + k_3)(\alpha x + \beta) = \dfrac{c}{d}(\alpha^2 x^2 + \beta^2 + 2\alpha\beta x) + \dfrac{k_1}{d}$.
We thus obtain general relations among all constants, given by

$$\begin{cases} \frac{c}{d}(k_4\alpha - \alpha^2) = 0 \\ \alpha + \frac{c}{d}k_3\beta - \frac{c}{d}\beta^2 - \frac{k_1}{d} = 0 \\ \beta k_4 + \alpha k_3 - 2\alpha\beta = 0. \end{cases}$$

These are now options, of each just one has not yet been discussed. If we pose $\alpha = 0$ or $\alpha = k_4 = 0$ we turn back to the first case. The other option is to let $\alpha = k_4$ and $\beta = k_3$, moreover assuming $k_2 = 0$, which satisfies also the second equation of the system. Therefore the particular solution becomes $u_p = \frac{k_1}{d}x + k_3$.
Higher polynomial terms (x^2, x^3, etc) do not yield any solution.
Note that the detailed calculations are presented in the appendix, whereas here we have reported only the main steps. We below report the three solutions, case by case.

Case 1: $\mathbf{u_p = 0}$ and $\mathbf{k_1 = 0}$

Equation (3.9), with these values, becomes

$$u' + \frac{c}{d}(k_4 x + k_3)u = \frac{c}{d}u^2$$

and u_p is trivially a solution. Since in this case $u_p = 0$, find u_1 means find the general solution u.
Through the calculations, imposing $u(0) = 1$ and the boundary condition $d\frac{\partial u}{\partial x}\Big|_{x=0} - cv(0)u(0) = 0$, we obtain the following solution for $u(x)$:

$$u(x) = \frac{e^{\frac{c}{d}(\frac{k_2}{d}\frac{x^2}{2}+x)}}{1 + \frac{\sqrt{c}}{\sqrt{d}\sqrt{-k_2}}e^{\frac{c}{-2k_2}}\sqrt{\frac{\pi}{2}}\left(\text{erf}\left[\frac{\sqrt{c}}{\sqrt{2}}\frac{-1}{\sqrt{-k_2}}\right] - \text{erf}\left[\frac{\sqrt{c}}{\sqrt{2}}\frac{-1-\frac{k_2}{d}x}{\sqrt{-k_2}}\right]\right)}, \qquad (3.11)$$

where erf(x) is defined as:

$$\text{erf}(x) = \frac{2}{\sqrt{\pi}}\int_0^x e^{-t^2}dt.$$

An explicit expression for $u(x)$, not depending on any parameter k_i, is complex to obtain, as well as it is not possible to enforce the condition $\int_0^1 u(x)dx = 1$ analytically. Also, it is important to realise that the imposition of such condition on the analytic solution is fundamentally different than the way we enforced the same condition in the numerical integration previously discussed for Eq. (2.13).

Case 2: $\mathbf{u_p = \alpha}$, $\mathbf{k_4 = 0}$ and $\boldsymbol{\alpha} = \dfrac{\mathbf{ck_3 \pm \sqrt{c^2k_3^2 - 4ck_1}}}{\mathbf{2c}}$

First, note that $k_4 = 0$ means $k_1 = k_2$. Also, it is easily verified that $k_3 = -1$, so equation (3.9) becomes

$$u' - \frac{c}{d}u = \frac{c}{d}u^2 + \frac{k_1}{d}. \tag{3.12}$$

The particular solution, u_p, satisfies (3.12) and imposing the integral constraint, we obtain the $u(x)$ that solves the above equation.

$$u(x) = \frac{e^{\frac{c}{d}(1+2\alpha)x}(1+2\alpha)}{\frac{e^{\frac{c}{d}(2+\alpha)}-1}{(1+2\alpha)(e^{(1-\alpha)\frac{c}{d}}-1)}(1+2\alpha) - e^{\frac{c}{d}(1+2\alpha)x}} + \alpha. \tag{3.13}$$

Case 3: $\mathbf{u_p = \alpha x + \beta}$ with $\boldsymbol{\alpha} = \mathbf{k_4} = \dfrac{\mathbf{k_1}}{\mathbf{d}}$, $\mathbf{k_2 = 0}$ and $\boldsymbol{\beta}$= $\mathbf{k_3}$

Finally, in this last case, the particular solution takes the form

$$u_p = \frac{k_1}{d}x + k_3.$$

Thus, the equation to solve becomes

$$u' + \frac{c}{d}\left(\frac{k_1}{d}x + k_3\right)u = \frac{c}{d}u^2 + \frac{k_1}{d}.$$

Applying the same procedure of the above cases, calculations lead to the following solution:

$$\begin{aligned} u(x) = {} & \frac{2c - ck_3(1-k_3) - (k_3-1)^2}{d}x + k_3 \\ & + \left(e^{\frac{c}{d}\left(\frac{2c-ck_3(1-k_3)-(k_3-1)^2}{2d}x^2 + k_3x\right)}\right) \Bigg/ \left(c_1 - \frac{\sqrt{c}}{\sqrt{2c - ck_3(1-k_3) - (k_3-1)^2}}\cdot\right. \\ & \left. \cdot\, e^{-\frac{ck_3^2}{2(2c-ck_3(1-k_3)-(k_3-1)^2)}}\sqrt{\frac{\pi}{2}}\,\mathrm{erfi}\left[\sqrt{\frac{c}{2}}\frac{dk_3 + (2c - ck_3(1-k_3) - (k_3-1)^2)x}{d\sqrt{2c - ck_3(1-k_3) - (k_3-1)^2}}\right]\right), \end{aligned} \tag{3.14}$$

where erfi(x) is defined as:

$$\mathrm{erfi}(x) = \frac{2}{\sqrt{\pi}}\int_0^x e^{t^2}dt.$$

We can see that the solution u(x) is considerably complex, and it is not possible to define a value for k_3 imposing the conservation of the area under the curve.
Similarly to the case of density $u(x)$ we can find the solution of the advection-diffusion equation with respect to $v(x)$:

$$v' - \frac{c}{d}v^2 - \frac{c}{d}(k_4 x + k_3)v = \frac{k_2}{d},$$

which is a Riccati equation too. There are three possible particular solutions that consequently produce three general solutions for (3.10)and none of them could be expressed explicitly due to the complexity of calculations imposing the integral constraint. However their most explicit representation has been derived as follows, with detail of calculations in Appendix A.

Case 1: $\mathbf{v_p = 0}$ and $\mathbf{k_2 = 0}$ The solution is:

$$v(x) = \frac{e^{\frac{c}{d}\left(\frac{k_1 x^2}{2d} - x\right)}}{\frac{1}{2} + \frac{\sqrt{c}}{\sqrt{k_1}} e^{-\frac{c}{2k_1}} \sqrt{\frac{\pi}{2}} \left(\operatorname{erf}\left[\frac{\sqrt{c}}{\sqrt{2}} \frac{-1}{\sqrt{k_1}}\right] - \operatorname{erf}\left[\frac{\sqrt{c}}{\sqrt{2}} \frac{-1 + \frac{k_1}{d} x}{\sqrt{k_1}}\right] \right)} \tag{3.15}$$

Case 2: $\mathbf{v_p = \alpha}$, $k_4 = 0$ and $\boldsymbol{\alpha} = \dfrac{-\mathbf{ck_3} + \sqrt{\mathbf{c^2 k_3^2 - 4ck_2}}}{\mathbf{2c}}$
The solution is:

$$v(x) = \frac{(-1 + 2\alpha) e^{\frac{c}{d}(-1+2\alpha)x}}{(-1+2\alpha) \frac{-1 + e^{\frac{c}{d}\alpha}}{(-1+2\alpha)(e^{\frac{c}{d}(1-\alpha)} + 1)} - e^{\frac{c}{d}(-1+2\alpha)x}} + \alpha \tag{3.16}$$

Case 3: $\mathbf{v_p = \dfrac{k_2}{d} x - k_3}$ with $\mathbf{k_4 = 0}$
Finally, the more involved case is given by:

$$v(x) = e^{\frac{c}{d}\left(\frac{(ck_3(2+k_3)+2c)}{2d}x^2 - k_3 x\right)} \Bigg/ \Bigg(\frac{\sqrt{c}}{\sqrt{(ck_3(2+k_3)+2c)}} \tag{3.17}$$

$$\cdot\, e^{-\frac{ck_3^2}{2(ck_3(2+k_3)+2c)}} \sqrt{\frac{\pi}{2}} \cdot \Bigg(\operatorname{erfi}\left[\sqrt{\frac{c}{2}} \frac{-k_3}{\sqrt{(ck_3(2+k_3)+2c)}} \right] -$$

$$- \operatorname{erfi}\left[\sqrt{\frac{c}{2}} \frac{-dk_3 + (ck_3(2+k_3)+2c)x}{d\sqrt{(ck_3(2+k_3)+2c)}} \right] \Bigg) + \frac{1}{2+k_3} \Bigg) +$$

$$+ \frac{(ck_3(2+k_3)+2c)}{d} x - k_3.$$

We now examine some plots of the analytical solutions derived previously. In particular we focus on Eq. (3.13), where k_1 is the only remaining free parameter. For better generality, we explore a larger variety of cases case where the initial conditions are not fixed and parameters have freedom to be set differently.

A comparison between the analytical solutions of the Riccati equation (Fig. 3.1) and the numerical results of the PDE system (next section) reveals a remarkably consistent behaviour. Specifically, when the PDE system approaches its final time evolution at t=10, the spatial distribution of the koala densities is similar to the profiles predicted by the analytical solution.

It is worth noting that this analytical solution was derived under the sole constraint of the normalisation integral equal to 1, without being strictly bound by the initial conditions. From calculations, we can see that imposing $k_3 = -1$ is equivalent to enforcing the conditions $u(0) = 1$ and $v(0) = 2$. Thus, panel a) of Fig. 3.1 accurately represents the solution (3.13), where only the parameter k_1 remains free. Panel b) still shows resemblance with case a), whereas the other panels show different behaviours for initial $u(0)$ where koala U shows a large density at the proximity of the origin. The curves in panel d) are quite remarkably in line with the numerically integrated ODEs for the case of both koalas close to the same tree. Interestingly, their range, as for the cases of the rest of the panels, is not entirely positive, in agreement with the truncation procedure we introduce in the previous section.

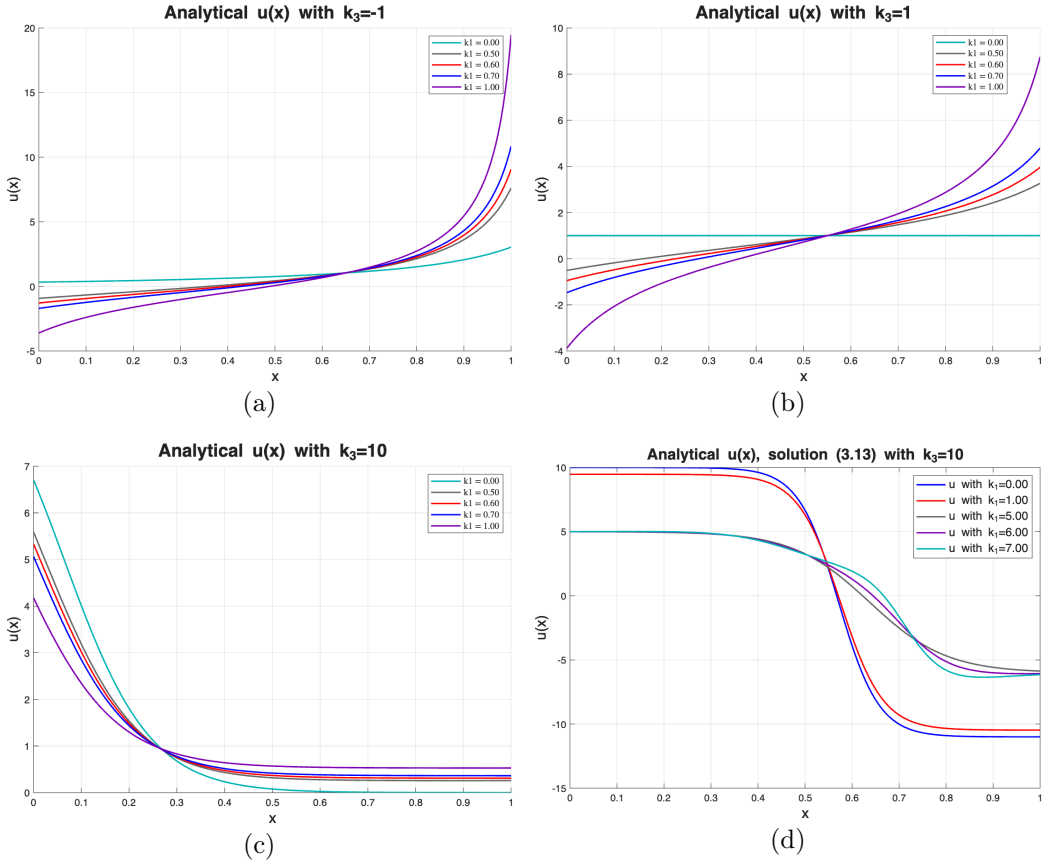

Figure 3.1: Analytical solution u considering the second particular solution of Riccati equation. (see Eq. (3.13))

3.2 Numerical solution for the PDEs

Let us now consider the one dimensional version of the full system (2.6):

$$\begin{cases} \dfrac{\partial u}{\partial t}(x,t) = d\dfrac{\partial^2 u}{\partial x^2}(x,t) - c\dfrac{\partial}{\partial x}(u(x,t)q(x,t)) \\ \dfrac{\partial v}{\partial t}(x,t) = d\dfrac{\partial^2 v}{\partial x^2}(x,t) - c\dfrac{\partial}{\partial x}(v(x,t)p(x,t)) \\ \dfrac{\partial p}{\partial t}(x,t) = u(x,t)(1+mq(x,t)) - p(x,t) \\ \dfrac{\partial q}{\partial t}(x,t) = v(x,t)(1+mp(x,t)) - q(x,t). \end{cases} \tag{3.18}$$

Here we analyse a slightly different version of the problem described for the ODEs. We solve the equations numerically, and impose the integral

constraint a posteriori, normalising the curves obtained at each time step without defining any auxiliary variable, as done for the ODEs system. The structure of the ODE allowed to impose both the fixed boundary conditions ($u(0) = 1$ and $v(1) = 2$) and the Neumann boundary conditions.

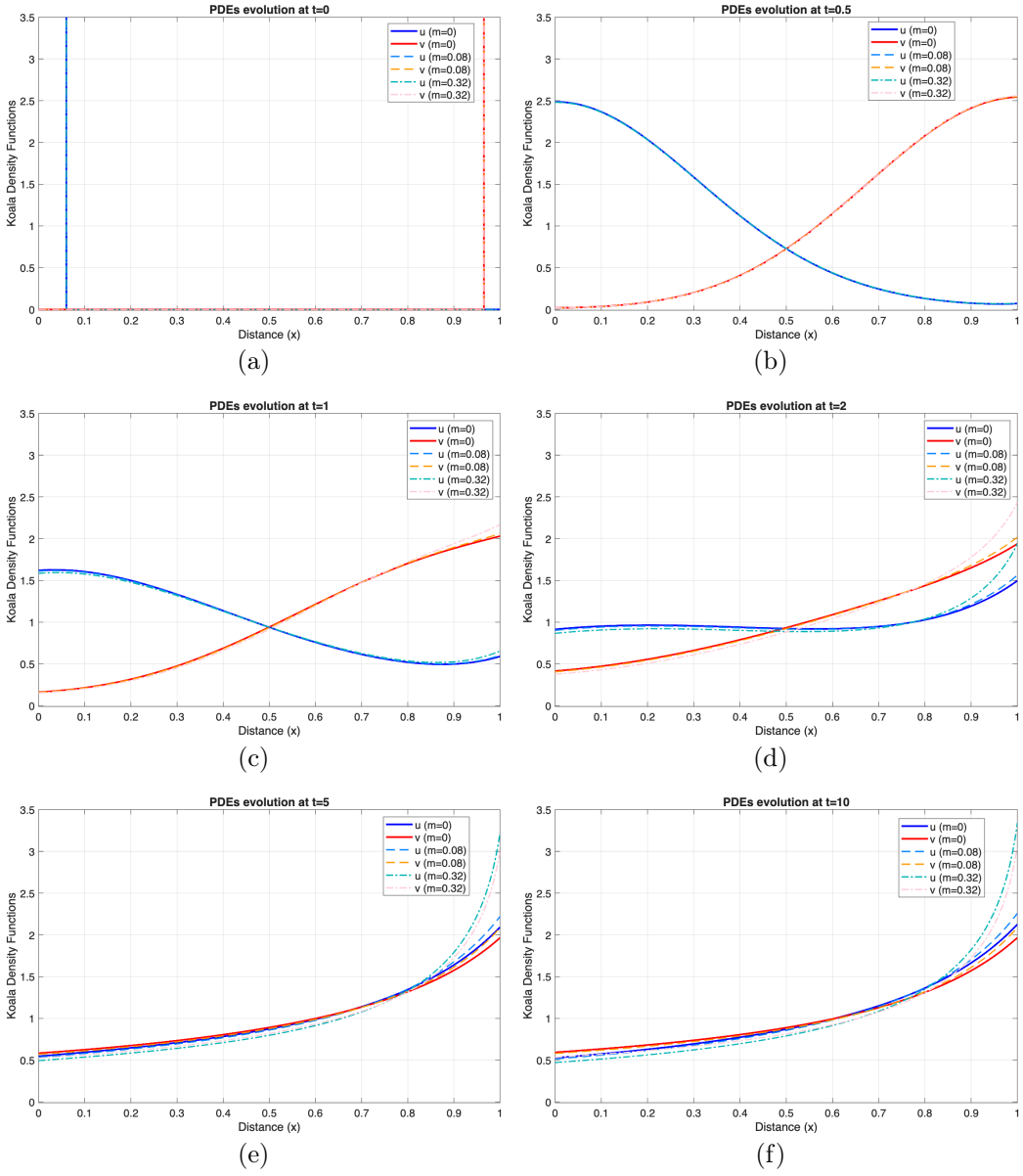

Figure 3.2: Evolution of the PDEs system (3.18) at selected times (t=0, 0.5, 1, 2, 5, 10), with diffusive parameter $d = 0.1$, advection coefficient $c = 0.2$. The curves represent pairs of solutions $u(x,t)$, $v(x,t)$ associated with different m.

Here we consider the initial condition as Dirac delta functions $u(x,0) = \delta(x-0.05)$ and $v(x,0) = \delta(x-0.99)$ with narrow bases ($b_u = 0.1, b_v = 0.05$) and heights 10 and 20, respectively. This gives an approximate area at $t = 0$ that resembles the conditions of the ODEs at the edge of the domain.

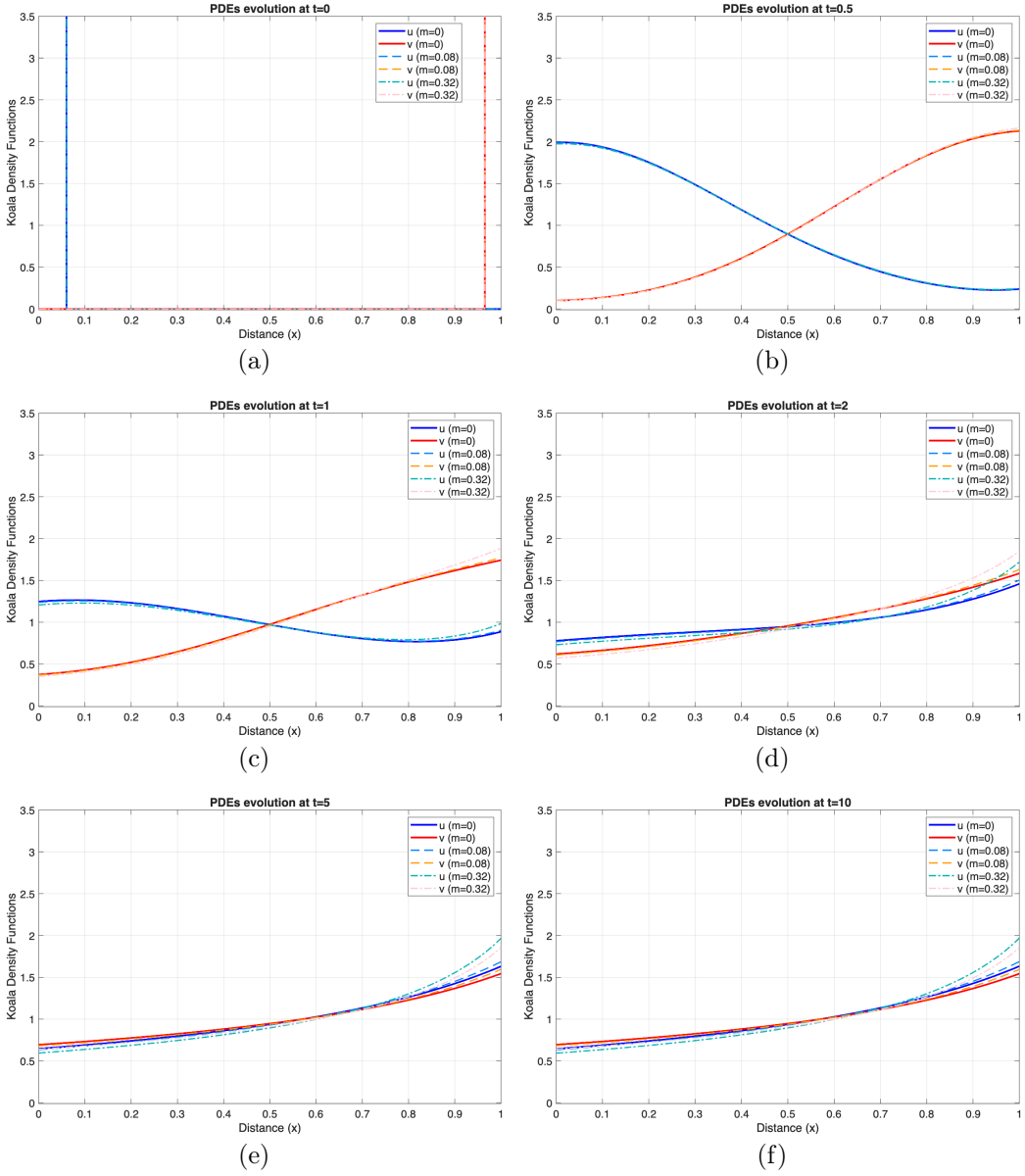

Figure 3.3: Evolution of the PDEs system (3.18) at selected times (t=0, 0.5, 1, 2, 5, 10), with diffusive parameter $d = 0.15$, advection coefficient $c = 0.2$. The curves represent pairs of solutions associated with different m.

In the these figures, we illustrate the evolution of the solutions at selected time instants (t=0,0.5,1,2,5,10) as they approach the steady-state, with different parameters d and m. Despite the simplified version of the system, the resulting curves exhibit interesting behaviours.
In Figs. 3.2-3.4, specifically at t=0.5,1 (panels (b) and (c)), the curves show a similar behaviour to that observed in Figs. 1.2 and 1.3. So, at early times in the evolution, this model shows koalas that do not behave that dissimilarly than the case of wolves in one dimension. Over time, however, the effect of the scent decays, and the curves flatten, nearly clustering together into a single profile. At higher values of diffusivity d, solutions show extensive overlap, as the sensitivity to the marking response has a minor effect, consistent with previous observations of the ODE system.
As diffusivity increases, dynamics also resemble simple, quasi-linear profiles, as the changes from $d = 0.1$ to $d = 0.19$ clearly show (see Figs. 3.2-3.4).
PDE solutions behave differently from ODEs solutions: PDE systems provide monotonic results that remain similar to each other even with different parameters. The primary cause of this discrepancy is the removal of the fixed boundary condition: the endpoints are no longer constrained at given values. In addition, specifically where m is large, advection has a great impact on the resultant ODE solutions, providing a substantial difference between the curves at the end of the interval. Here the behaviour of u and v remains similar because the endpoints of the domain are not fixed, and the no flux boundary conditions allow for solutions that can "slide" along the end and the beginning of the boundary.
It is worth noting that the cases analysed reach a steady-state solution around $t = 10$. Under the chosen nondimensionalisation, t=10 corresponds to 10 days; this timescale appears biologically plausible, although it would require empirical validation and it can be highly dependent on multiple factors, such as terrain, proximity to urbanisation, and so on.
and it is consistent with biological reality.
This is means is that, after 10 days, koalas have reached an equilibrium where the distributions are basically identical and there is no more "memory" of the initial conditions.
This PDE captures the time evolution of interactions in a habitat where boundaries do not intrinsically limit and constrain the animals' motilities.
Setting boundary conditions $u(0)$, $v(0)$, $v(1)$ (or similar) instead captures a spatial distribution influenced by factors that limit their habitat, such as anthropogenic infrastructure like roads and bridges. It could be interesting to understand a useful approach capable of taking into consideration other factors of the environment such as the quality and spatial distribution of trees or the presence of traffic in the contest of the PDE system. Nonetheless, these

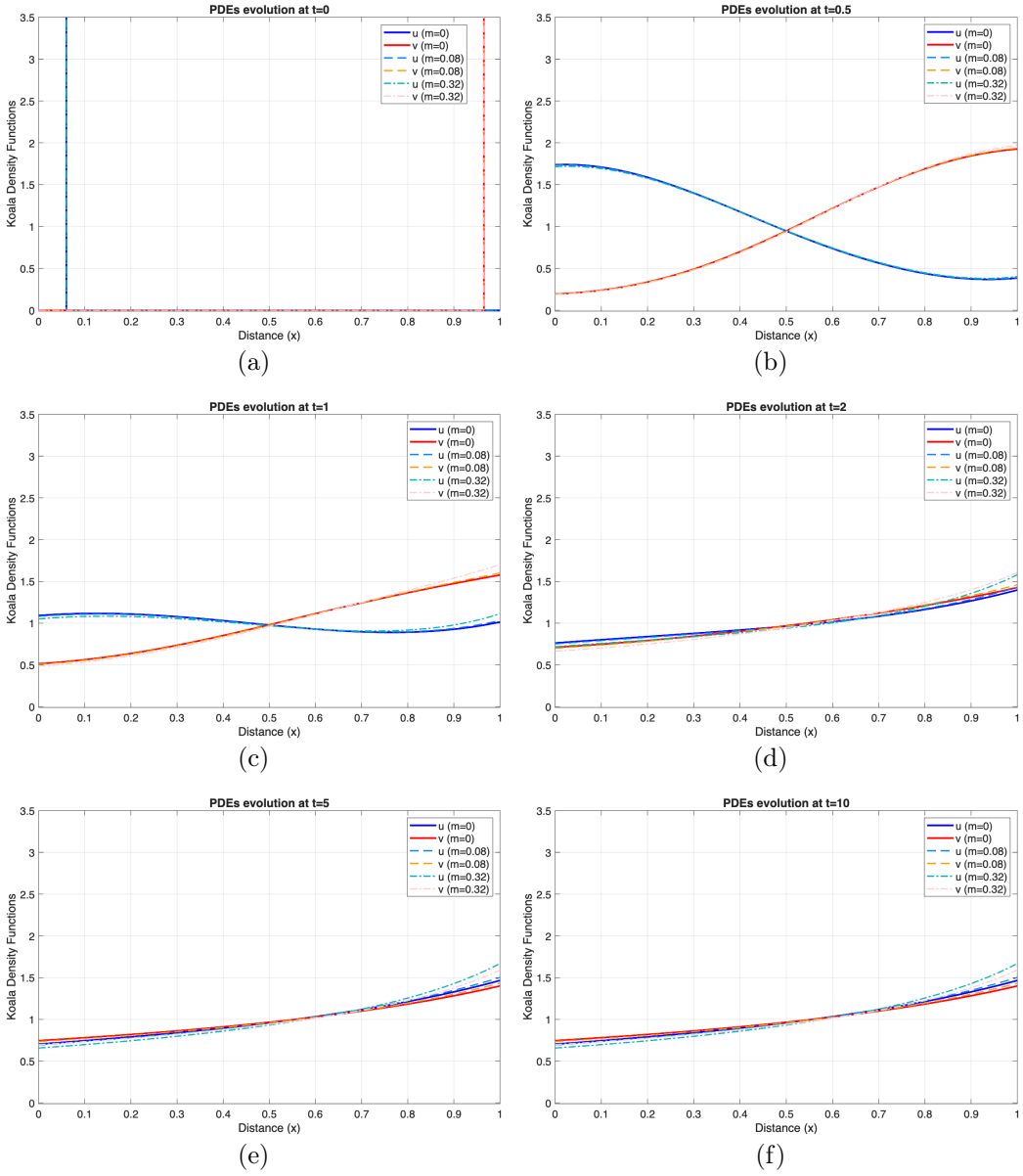

Figure 3.4: Evolution of the PDEs system (3.18) at selected time (t=0, 0.5, 1, 2, 5, 10), with diffusive parameter $d = 0.19$, advection coefficient $c = 0.2$. The curves represent pairs of solutions associated with different m.

results represent a good depiction of koalas interacting, where, not facing obstacles or limitations, they have homogeneous and monotonic home ranges. This seems in line with cases in the wild where the number of individuals is low and the space to explore for food search is sufficiently large. In those habitats, home ranges are usually quite extended and contacts or overlaps are not so common, as some data clearly show at Karawatha Forest Park, south Brisbane (Lollback et al., 2018).

Chapter 4

Conclusion and outlook

In conclusion, this thesis shows significant insights into koala spatial dynamics within a one-dimensional domain. Specifically, in Chapter 2 we understand the critical role of the scent marks for koala movement patterns. The results presented confirm that koalas dynamics is influenced by the attraction toward resources and by repulsion from conspecifics. Given the low motility of koalas, the numerical ODE solutions confirm a low tendency to encounters, in particular when the individuals exhibit high avoidance toward foreign scent marks.
The importance of these results lies in their potential application to repopulation and management strategies. One of the most compelling aspects is their ability to qualitatively match empirical observations, such as those from Cape Otway (2025). The observed "affiliative" behaviors between young males can be interpreted through our model by assuming higher diffusivity and lower marking sensitivity. This suggests that the age of individuals could be important in defining the magnitude of avoidance and diffusion in our model. Young individuals seem to have a lower sensitivity to foreign scent marks and a consequently lower marking response. This likely facilitates the social interactions observed in Cape Otway population.
However, it is worth noting that these results do not yet consider any other external factor that alters the movement decisions of an individual, such as food availability or habitat quality. A further step toward more biological realism would be to modify the assumption of the one dimensional space domain. In this study we considered a uniformly accessible spatial domain where the movements are mainly driven by interactions with conspecifics and by advection toward a particular tree; however natural habitats are characterised by a non-uniform distribution of resources or obstacles that could significantly alter individual movement decisions. For instance, the model could be extended to define particular areas within the interval domain where

a higher abundance of resources create an incentive to "staying". In these areas, a koala might spend a larger amount of time foraging, temporarily stopping its trajectory towards a more distant target. Mathematically, this behaviour could be incorporated by introducing spatially varying magnitudes of advective and diffusive coefficients; for example, the magnitude of the diffusive coefficient could be reduced in resource-rich zones to simulate lower motility.

Another natural development is to extend this study to a two dimensional model in which habitat characteristics could be incorporated. Our model shows that the locations of trees and the geometry of the spatial domain are crucial to understand the distribution and the consequent potential interactions of koalas in the environment. From a conservation perspective, a simple "headcount" of trees is insufficient for effective habitat management. Moving to a two-dimensional domain requires a generalized formulation of the system, replacing the 1D derivatives with the Laplacian operator for diffusion and the divergence of the flux for advection. Better understanding of koalas' home ranges is essential for a proper conservation of these fascinating creatures.

Appendix A

Analytical solutions for the one-dimensional ODE system

Let us show more details on the techniques used for arriving at an analytical solution for the home range problem. First, we look at the case for equation (3.9), or population $u(x)$.

Case 1: $\mathbf{u_p = 0}$ and $\mathbf{k_1 = 0}$

The expression becomes

$$u' + \frac{c}{d}(k_4 x + k_3)u = \frac{c}{d}u^2$$

and u_p easily satisfies it: since in this case $u_p = 0$, finding u_1 means arriving at the general solution u. This implies we have to now solve:
Let's find the solution for the following equation.

$$u_1' + \frac{c}{d}(k_4 x + k_3)u_1 = \frac{c}{d}u_1^2 \tag{A.1}$$

We put

$$y := u_1^{-1}$$

and so

$$y' = -\frac{u_1'}{u_1^2}.$$

Substituting these variables in (A.1) and dividing for u_1^2, the equation becomes

$$y' - \frac{c}{d}(k_4 x + k_3)y = -\frac{c}{d}.$$

This is a linear ODE of first order, hence the solution is given by:

$$y(x) = e^{-A(x)} \left(c_1 + \int f(x) e^{A(x)} dx \right),$$

where, in our case, we have

$$A(x) = \int -\frac{c}{d}(k_4 x + k_3) dx = -\frac{c}{d} \left(k_4 \frac{x^2}{2} + k_3 x \right)$$

and

$$f(x) = -\frac{c}{d}.$$

Combining both terms, we have:

$$y(x) = e^{\frac{c}{d}\left(k_4 \frac{x^2}{2} + k_3 x\right)} \left(c_1 + \int -\frac{c}{d} e^{-\frac{c}{d}\left(k_4 \frac{x^2}{2} + k_3 x\right)} dx \right)$$

$$= e^{\frac{c}{d}\left(k_4 \frac{x^2}{2} + k_3 x\right)} \left(c_1 - \frac{\sqrt{c}}{\sqrt{d}\sqrt{k_4}} e^{\frac{ck_3^2}{2dk_4}} \sqrt{\frac{\pi}{2}} \operatorname{erf}\left[\frac{\sqrt{c}}{\sqrt{2}} \frac{k_3 + k_4 x}{\sqrt{d}\sqrt{k_4}} \right] \right).$$

Now, remembering that $u = u_1$ and $u_1 = y^{-1}$, we arrive at

$$u(x) = \frac{e^{-\frac{c}{d}\left(k_4 \frac{x^2}{2} + k_3 x\right)}}{c_1 - \frac{\sqrt{c}}{\sqrt{d}\sqrt{k_4}} e^{\frac{ck_3^2}{2dk_4}} \sqrt{\frac{\pi}{2}} \operatorname{erf}\left[\frac{\sqrt{c}}{\sqrt{2}} \frac{k_3 + k_4 x}{\sqrt{d}\sqrt{k_4}} \right]}.$$

We can impose initial condition $u(0) = 1$ and see that

$$1 = \frac{1}{c_1 - \frac{\sqrt{c}}{\sqrt{d}\sqrt{k_4}} e^{\frac{ck_3^2}{2dk_4}} \sqrt{\frac{\pi}{2}} \operatorname{erf}\left[\frac{\sqrt{c}}{\sqrt{2}} \frac{k_3}{\sqrt{d}\sqrt{k_4}} \right]}.$$

Thus

$$c_1 = 1 + \frac{\sqrt{c}}{\sqrt{d}\sqrt{k_4}} e^{\frac{ck_3^2}{2dk_4}} \sqrt{\frac{\pi}{2}} \operatorname{erf}\left[\frac{\sqrt{c}}{\sqrt{2}} \frac{k_3}{\sqrt{d}\sqrt{k_4}} \right]$$

and

$$u(x) = \frac{e^{-\frac{c}{d}\left(k_4 \frac{x^2}{2} + k_3 x\right)}}{1 + \frac{\sqrt{c}}{\sqrt{d}\sqrt{k_4}} e^{\frac{ck_3^2}{2dk_4}} \sqrt{\frac{\pi}{2}} \left(\operatorname{erf}\left[\frac{\sqrt{c}}{\sqrt{2}} \frac{k_3}{\sqrt{d}\sqrt{k_4}} \right] - \operatorname{erf}\left[\frac{\sqrt{c}}{\sqrt{2}} \frac{k_3 + k_4 x}{\sqrt{d}\sqrt{k_4}} \right] \right)}.$$

Remind that erf(x) is defined as

$$\operatorname{erf}(x) = \frac{2}{\sqrt{\pi}} \int_0^x e^{-t^2} dt.$$

To find k_3 we can now use the condition we have on the derivative for $x = 0$ and the initial conditions: $\frac{\partial u}{\partial x}(0) = \frac{c}{d}u(0)v(0) = 2\frac{c}{d}$.
To simplify notation of the derivative of $u(x)$ we call

$$a(x) = -\frac{c}{d}(k_4 x + k_3),$$

$$A(x) = \int a(x) = -\frac{c}{d}\left(k_4\frac{x^2}{2} + k_3 x\right),$$

$$B = \frac{ck_3^2}{2dk_4},$$

$$D(x) = 1 + \frac{\sqrt{c}}{\sqrt{d}\sqrt{k_4}}e^{\frac{ck_3^2}{2dk_4}}\sqrt{\frac{\pi}{2}}\left(\text{erf}\left[\frac{\sqrt{c}}{\sqrt{2}}\frac{k_3}{\sqrt{d}\sqrt{k_4}}\right] - \text{erf}\left[\frac{\sqrt{c}}{\sqrt{2}}\frac{k_3 + k_4 x}{\sqrt{d}\sqrt{k_4}}\right]\right)$$

and remembering that

$$\frac{\partial(\text{erf}[f(x)])}{\partial x} = \frac{2}{\sqrt{\pi}}e^{-f(x)^2}f'(x),$$

we have an expression for the firs derivative as follows:

$$u'(x) = \frac{a(x)e^{A(x)}D + e^{A(x)}\left(\frac{\sqrt{c}}{\sqrt{d}\sqrt{k_4}}e^B\frac{\sqrt{\pi}}{\sqrt{2}}\frac{\sqrt{c}}{\sqrt{d}}e^{\frac{-c(k_3=k_4x)^2}{2dk_4}}\sqrt{k_4}\sqrt{\frac{2}{\pi}}\right)}{D^2}$$
$$= \frac{a(x)e^{A(x)}D + e^{A(x)}\left(\frac{c}{d}e^B e^{\frac{-c(k_3=k_4x)^2}{2dk_4}}\right)}{D^2}.$$

We note that

$$a(0) = -\frac{c}{d}k_3,$$

$$A(0) = 0,$$

$$B = \frac{ck_3^2}{2dk_4},$$

$$D(0) = 1.$$

Substituting those constant. we find:

$$u'(0) = \frac{-\frac{c}{d}k_3 + (\frac{c}{d}e^B e^{-B})}{1} = \frac{c}{d}(-k_3 + 1)$$

$$\implies \frac{c}{d}(-k_3 + 1) = 2\frac{c}{d} \implies k_3 = -1.$$

We can thus substitute the value of $k_3 = -1$ in $u(x)$

$$u(x) = \frac{e^{-\frac{c}{d}(k_4 \frac{x^2}{2} - x)}}{1 + \frac{\sqrt{c}}{\sqrt{d}\sqrt{k_4}} e^{\frac{c}{2dk_4}} \sqrt{\frac{\pi}{2}} \left(\text{erf}\left[\frac{\sqrt{c}}{\sqrt{2}} \frac{-1}{\sqrt{d}\sqrt{k_4}}\right] - \text{erf}\left[\frac{\sqrt{c}}{\sqrt{2}} \frac{-1+k_4 x}{\sqrt{d}\sqrt{k_4}}\right]\right)}.$$

Remembering that $k_4 = \frac{k_1 - k_2}{d}$ and, in this case $k_1 = 0$, the only parameter left to find is k_2, which still appears in the expression for $u(x)$, i.e.:

$$u(x) = \frac{e^{\frac{c}{d}(\frac{k_2}{d}\frac{x^2}{2} + x)}}{1 + \frac{\sqrt{c}}{\sqrt{d}\sqrt{-k_2}} e^{\frac{c}{-2k_2}} \sqrt{\frac{\pi}{2}} \left(\text{erf}\left[\frac{\sqrt{c}}{\sqrt{2}} \frac{-1}{\sqrt{-k_2}}\right] - \text{erf}\left[\frac{\sqrt{c}}{\sqrt{2}} \frac{-1-\frac{k_2}{d}x}{\sqrt{-k_2}}\right]\right)},$$

where

$$\text{erf}(x) = \frac{2}{\sqrt{\pi}} \int_0^x e^{-t^2} dt.$$

An explicit expression for $u(x)$, not depending on any parameter k_i, is complex to obtain explicitly, and has to be determined by invoking the normalisation condition for $u(x)$ over the domain. Alternatively, numerical integration can be considered.

Case 2: $\mathbf{u_p = \alpha}$, $\mathbf{k_4 = 0}$ and $\boldsymbol{\alpha} = \frac{\mathbf{ck_3 \pm \sqrt{c^2 k_3^2 - 4ck_1}}}{\mathbf{2c}}$

First we observe that Eq. (3.7) is true for all $x \in [0, 1]$, in particular for $x = 0$. Thus, setting $u(0) = 1$ and $v(0) = 2$, we obtain an expression for k_3:

$$-1 = u(0) - v(0) = k_3$$

and the equation (3.9) becomes:

$$u' - \frac{c}{d}u^2 - \frac{c}{d}u = \frac{k_1}{d}. \tag{A.2}$$

Both the general and the particular solution, u and u_p respectively, satisfy (A.2). Since $u = u_1 + u_p$, we have

$$u_1' - \frac{c}{d}(u_1 + \alpha) = \frac{c}{d}(\alpha^2 + u_1^2 + 2\alpha u_1) + \frac{k_1}{d},$$

but also

$$u_1' - \frac{c}{d}(1+2\alpha)u_1 = \frac{c}{d}u_1^2.$$

We define

$$y := u_1^{-1} \Longrightarrow y' = -\frac{u_1'}{u_1}$$

and by making this change of variable u_1 and dividing for u_1^2 we obtain:

$$y' + \frac{c}{d}(2\alpha+1)y = -\frac{c}{d}.$$

This is again a linear ODE of the first order and the solution has the form:

$$y(x) = e^{-A(x)}\left(c_1 + \int f(x)e^{A(x)}dx\right),$$

where

$$A(x) = \int \frac{c}{d}(1+2\alpha)dx = \frac{c}{d}(1+2\alpha)x$$

and

$$f(x) = -\frac{c}{d}.$$

Putting all together:

$$\begin{aligned} y(x) &= e^{-\frac{c}{d}(1+2\alpha)x}\left(c_1 + \int -\frac{c}{d}e^{\frac{c}{d}(1+2\alpha)x}dx\right) \\ &= e^{-\frac{c}{d}(1+2\alpha)x}\left(c_1 - \frac{e^{\frac{c}{d}(1+2\alpha)x}}{1+2\alpha}\right). \end{aligned}$$

Now, knowing that $u = u_p + u_1 = \alpha + u_1$ and $u_1 = y^{-1}$,

$$u(x) = \frac{e^{\frac{c}{d}(1+2\alpha)x}(1+2\alpha)}{c_1(1+2\alpha) - e^{\frac{c}{d}(1+2\alpha)x}} + \alpha. \tag{A.3}$$

We can apply the integral constraint now to have:

$$\begin{aligned} 1 &= \int_0^1 \left(\frac{e^{\frac{c}{d}(1+2\alpha)x}(1+2\alpha)}{c_1(1+2\alpha) - e^{\frac{c}{d}(1+2\alpha)x}} + \alpha\right)dx = \\ &= \left[-\frac{d}{c}\log\left(c_1(1+2\alpha) - e^{\frac{c}{d}(1+2\alpha)x}\right) + \alpha x\right]_0^1 = \\ &= \frac{d}{c}\left(\log(c_1(1+2\alpha)-1) - \log\left(c_1(1+2\alpha) - e^{\frac{c}{d}(1+2\alpha)}\right)\right) + \alpha = \\ &= \frac{d}{c}\log\left(\frac{c_1(1+2\alpha)-1}{c_1(1+2\alpha) - e^{\frac{c}{d}(1+2\alpha)}}\right) + \alpha. \end{aligned}$$

Thus, after some algebra,

$$(1-\alpha)\frac{c}{d} = \log\left(\frac{c_1(1+2\alpha)-1}{c_1(1+2\alpha)-e^{\frac{c}{d}(1+2\alpha)}}\right)$$

$$e^{(1-\alpha)\frac{c}{d}} = \frac{c_1(1+2\alpha)-1}{c_1(1+2\alpha)-e^{\frac{c}{d}(1+2\alpha)}}$$

$$e^{\frac{c}{d}(2+\alpha)} - 1 = c_1(1+2\alpha)(e^{(1-\alpha)\frac{c}{d}} - 1).$$

We can now solve for c_1, as follows:

$$c_1 = \frac{e^{\frac{c}{d}(2+\alpha)} - 1}{(1+2\alpha)\left(e^{(1-\alpha)\frac{c}{d}} - 1\right)}$$

Finally, we are able to substitute this expression for c_1 in the equation (A.3):

$$u(x) = \frac{e^{\frac{c}{d}(1+2\alpha)x}(1+2\alpha)}{\frac{e^{\frac{c}{d}(2+\alpha)}-1}{(1+2\alpha)\left(e^{(1-\alpha)\frac{c}{d}}-1\right)}(1+2\alpha) - e^{\frac{c}{d}(1+2\alpha)x}} + \alpha. \tag{A.4}$$

In similar fashion to case 1, the explicit solution $u(x)$ for this second case, requires to determine the value for k_1, since α depends on this parameter. The value of k_1 is on the right hand side of equation (3.9) and determines hoe the ODEs are parametrised (see Eq. (3.5)).

Case 3: $\mathbf{u_p = \alpha x + \beta}$ with $\boldsymbol{\alpha} = \mathbf{k_4} = \frac{\mathbf{k_1}}{\mathbf{d}}$, $\mathbf{k_2 = 0}$ and $\boldsymbol{\alpha} = \mathbf{k_3}$

The particular solution in this case is

$$u_p = \frac{k_1}{d}x + k_3;$$

and the equation to solve becomes

$$u' + \frac{c}{d}\left(\frac{k_1}{d}x + k_3\right)u = \frac{c}{d}u^2 + \frac{k_1}{d}.$$

Again, we search $u = u_1 + u_p$ that satisfies the expression above, knowing that even the particular solution satisfies the same equation:

$$u_1' + u_p' + \frac{c}{d}\left(\frac{k_1}{d}x + k_3\right)(u_1 + u_p) = \frac{c}{d}\left(u_1^2 + u_p^2 + 2u_1u_p\right) + \frac{k_1}{d},$$

so

$$u_1' + \frac{c}{d}\left(\frac{k_1}{d}x + k_3\right)u_1 = \frac{c}{d}\left(u_1^2 + 2u_1\left(\frac{k_1}{d}x + k_3\right)\right)$$

$$u_1' - \frac{c}{d}\left(\frac{k_1}{d}x + k_3\right)u_1 = \frac{c}{d}u_1^2.$$

Now we put $u_1^{-1} = y$ and so $y' = -\frac{u_1'}{u_1^2}$, obtaining:

$$-y' - \frac{c}{d}\left(\frac{k_1}{d}x + k_3\right)y = \frac{c}{d}.$$

Equation

$$y' + \frac{c}{d}\left(\frac{k_1}{d}x + k_3\right)y = -\frac{c}{d}$$

has become a linear ODE of first order, thus the solution is:

$$y(x) = e^{-A(x)}\left(c_1 + \int -f(x)e^{A(x)}dx\right)$$

where

$$A(x) = \int \frac{c}{d}\left(\frac{k_1}{d}x + k_3\right)dx = \frac{c}{d}\left(\frac{k_1}{d}\frac{x^2}{2} + k_3x\right)$$

and

$$f(x) = -\frac{c}{d}.$$

Using a computer algebra system, such as Mathematica, gives the result:

$$y(x) = e^{-\frac{c}{d}\left(\frac{k_1}{2d}x^2 + k_3x\right)}\left(c_1 - \int \frac{c}{d}e^{\frac{c}{d}\left(\frac{k_1}{2d}x^2 + k_3x\right)}dx\right)$$

$$= e^{-\frac{c}{d}\left(\frac{k_1}{2d}x^2 + k_3x\right)}\left(c_1 - \frac{\sqrt{c}}{\sqrt{k_1}}e^{-\frac{ck_3^2}{2k_1}}\sqrt{\frac{\pi}{2}}\,\mathrm{erfi}\left[\sqrt{\frac{c}{2}}\frac{dk_3 + k_1x}{d\sqrt{k_1}}\right]\right).$$

Note that erfi(x) is defined as:

$$\mathrm{erfi}(x) = \frac{2}{\sqrt{\pi}}\int_0^x e^{t^2}dt.$$

Knowing that $y(x) = u_1^{-1}(x)$ and $u(x) = u_p(x) + u_1(x)$, we arrive at

$$u_1(x) = \frac{e^{\frac{c}{d}\left(\frac{k_1}{2d}x^2 + k_3x\right)}}{c_1 - \frac{\sqrt{c}}{\sqrt{k_1}}e^{-\frac{ck_3^2}{2k_1}}\sqrt{\frac{\pi}{2}}\,\mathrm{erfi}\left[\sqrt{\frac{c}{2}}\frac{dk_3 + k_1x}{d\sqrt{k_1}}\right]},$$

$$u(x) = \frac{k_1}{d}x + k_3 + \frac{e^{\frac{c}{d}\left(\frac{k_1}{2d}x^2 + k_3 x\right)}}{c_1 - \frac{\sqrt{c}}{\sqrt{k_1}} e^{-\frac{ck_3^2}{2k_1}} \sqrt{\frac{\pi}{2}} \operatorname{erfi}\left[\sqrt{\frac{c}{2}} \frac{dk_3 + k_1 x}{d\sqrt{k_1}}\right]}.$$

Imposing the initial condition $u(0) = 1$ we have

$$1 = k_3 + \frac{1}{c_1 - \frac{\sqrt{c}}{\sqrt{k_1}} e^{-\frac{ck_3^2}{2k_1}} \sqrt{\frac{\pi}{2}} \operatorname{erfi}\left[\sqrt{\frac{c}{2}} \frac{k_3}{\sqrt{k_1}}\right]}$$

$$c_1(1 - k_3) = (1 - k_3)\left(\frac{\sqrt{c}}{\sqrt{k_1}} e^{-\frac{ck_3^2}{2k_1}} \sqrt{\frac{\pi}{2}} \operatorname{erfi}\left[\sqrt{\frac{c}{2}} \frac{k_3}{\sqrt{k_1}}\right]\right) + 1,$$

allowing to solve for c_1:

$$c_1 = \frac{\sqrt{c}}{\sqrt{k_1}} e^{-\frac{ck_3^2}{2k_1}} \sqrt{\frac{\pi}{2}} \operatorname{erfi}\left[\sqrt{\frac{c}{2}} \frac{k_3}{\sqrt{k_1}}\right] + \frac{1}{1 - k_3}.$$

Substituting, we derive at the final expression:

$$u(x) = \frac{k_1}{d}x + k_3 + \frac{(1 - k_3) e^{\frac{c}{d}\left(\frac{k_1}{2d}x^2 + k_3 x\right)}}{(1 - k_3) \frac{\sqrt{c}}{\sqrt{k_1}} e^{-\frac{ck_3^2}{2k_1}} \sqrt{\frac{\pi}{2}} \left(\operatorname{erfi}\left[\sqrt{\frac{c}{2}} \frac{k_3}{\sqrt{k_1}}\right] - \operatorname{erfi}\left[\sqrt{\frac{c}{2}} \frac{dk_3 + k_1 x}{d\sqrt{k_1}}\right]\right) + 1}.$$

To find k_3 we can now use the condition we have on the derivative for $x = 0$ and the initial conditions: $\frac{\partial u}{\partial x}(0) = \frac{c}{d}u(0)v(0) = 2\frac{c}{d}$, similarly as we did previously. We have

$$u'(x) = \frac{k_1}{d} + \frac{(1 - k_3)\frac{c}{d}\left(\frac{k_1}{d}x + k_3\right) e^{\frac{c}{d}\left(\frac{k_1}{2d}x^2 + k_3 x\right)} D(x) - (1 - k_3) e^{\frac{c}{d}\left(\frac{k_1}{2d}x^2 + k_3 x\right)} D'(x)}{D^2(x)}$$

where

$$D(x) = (1 - k_3) \frac{\sqrt{c}}{\sqrt{k_1}} e^{-\frac{ck_3^2}{2k_1}} \sqrt{\frac{\pi}{2}} \left(\operatorname{erfi}\left[\sqrt{\frac{c}{2}} \frac{k_3}{\sqrt{k_1}}\right] - \operatorname{erfi}\left[\sqrt{\frac{c}{2}} \frac{dk_3 + k_1 x}{d\sqrt{k_1}}\right]\right) + 1.$$

Thus, deriving, we have:

$$D'(x) = (1 - k_3) \frac{\sqrt{c}}{\sqrt{k_1}} e^{-\frac{ck_3^2}{2k_1}} \sqrt{\frac{\pi}{2}} \left(-\frac{\sqrt{k_1}}{d} \sqrt{\frac{2}{\pi}} \sqrt{c} e^{\frac{c(dk_3 + k_1 x)^2}{2d^2 k_1}}\right)$$

$$= -\frac{1 - k_3}{d} e^{\frac{cx}{2d^2}(k_1 x + 2dk_3)},$$

$$D'(0) = \frac{k_3 - 1}{d},$$

$$D(0) = 1,$$

$$D^2(0) = 1,$$

and we use the constants above to write:

$$u'(0) = \frac{k_1}{d} + \frac{(1-k_3)\frac{c}{d}k_3 - (1-k_3)\frac{k_3-1}{d}}{1}$$

$$= \frac{k_1}{d} + \frac{c}{d}k_3(1-k_3) - (1-k_3)\frac{k_3-1}{d}.$$

Knowing that $u'(0) = \frac{2c}{d}$, we find

$$\frac{2c}{d} = \frac{1}{d}(k_1 + ck_3(1-k_3) + (k_3-1)^2)$$

which allows us to solve for k_1

$$k_1 = 2c - ck_3(1-k_3) - (k_3-1)^2.$$

Now we can substitute this result into the equation for $u(x)$ and find:

$$u(x) = \frac{2c - ck_3(1-k_3) - (k_3-1)^2}{d}x + k_3 + \\ + \frac{e^{\frac{c}{d}\left(\frac{2c-ck_3(1-k_3)-(k_3-1)^2}{2d}x^2 + k_3x\right)}}{c_1 - \frac{\sqrt{c}}{\sqrt{2c-ck_3(1-k_3)-(k_3-1)^2}}e^{-\frac{ck_3^2}{2(2c-ck_3(1-k_3)-(k_3-1)^2)}}\Lambda(x)}$$

where $\Lambda(x)$ is given by:

$$\Lambda(x) := \sqrt{\frac{\pi}{2}}\,\mathrm{erfi}\left[\sqrt{\frac{c}{2}}\frac{dk_3 + (2c - ck_3(1-k_3) - (k_3-1)^2)x}{d\sqrt{2c - ck_3(1-k_3) - (k_3-1)^2}}\right].$$

We can see that the equation found for u(x) is considerably more complex, therefore it is not possible to find a closed expression for k_3 imposing the conservation of the area in the domain.
Similarly to the case discussed for $u(x)$, we can obtain the solution of the advection-diffusion equation with respect to $v(x)$.

Now, the equation (3.10), is given by:

$$v' - \frac{c}{d}v^2 - \frac{c}{d}(k_4x + k_3)v = \frac{k_2}{d}.$$

We can see that this too is a Riccati equation, and the general solution v is given by the sum of a particular solution, called v_p, and another function v_1, as for $u(x)$

In parallel with previous cases, we have three different cases that could give us particular solution, depending on some parameters value. In the simplest case:

$v_p = \alpha \longrightarrow -\frac{c}{d}(k_4x + k_3)\alpha = \frac{c}{d}\alpha^2 + \frac{k_2}{d}$,

giving

$$\begin{cases} \frac{c}{d}k_4\alpha = 0 \\ ck_3\alpha + c\alpha^2 + k_2 = 0 \end{cases}.$$

We have two options, given by the following:

- $\alpha = 0$ and $k_2 = 0$
- $k_4 = 0 \longrightarrow k_1 = k_2$ and $\alpha = \frac{-ck_3 \pm \sqrt{c^2k_3^2 - 4ck_2}}{2c}$.

As a second possibility: $v_p = \alpha x + \beta \longrightarrow \alpha - \frac{c}{d}(k_4x + k_3)(\alpha x + \beta) = \frac{c}{d}(\alpha^2x^2 + \beta^2 + 2\alpha\beta x) + \frac{k_2}{d}$

$$\begin{cases} \frac{c}{d}(k_4\alpha + \alpha^2) = 0 \\ \alpha - \frac{c}{d}k_3\beta - \frac{c}{d}\beta^2 - \frac{k_2}{d} = 0 \\ \beta k_4 + \alpha k_3 + 2\alpha\beta = 0 \end{cases}$$

We have three options but just one we haven't already discussed. If we pose $\alpha = 0$ we go back to the point 1.1, if $\alpha = -k_4 = 0$ we get back to the point 1. The other option is to let $\alpha = -k_4 \neq 0$ and $\beta = -k_3$.and to satisfy also the second equation we need to put $k_1 = 0$. This means that $v_p = \frac{k_2}{d}x - k_3$. Let us proceed with the first case.

Case 1: $\mathbf{v_p = 0}$ and $\mathbf{k_2 = 0}$

The equation to solve is now

$$v' - \frac{c}{d}(k_4x + k_3)v = \frac{c}{d}v^2$$

Again, v_p satisfies it and now we want to find the general solution $v = v_1 + v_p$. Since, in our case, $v = v_1 + 0$, we only need to find v_1 that satisfies the equation.

$$v_1' - \frac{c}{d}(k_4x + k_3)v_1 = \frac{c}{d}v_1^2$$

In order to solve this equation we put

$$y = v_1^{-1}$$

and so

$$y' = -\frac{v_1'}{v_1^2}.$$

Now, substituting in the equation and dividing it for v_1^2:

$$y' + \frac{c}{d}(k_4 x + k_3)y = -\frac{c}{d}$$

and this is a linear ODE of first order. As usual:

$$y(x) = e^{-A(x)}\left(c_1 + \int -f(x)e^{A(x)}dx\right),$$

where

$$A(x) = \int \frac{c}{d}(k_4 x + k_3)dx = \frac{c}{d}\left(k_4\frac{x^2}{2} + k_3 x\right)$$

and

$$f(x) = -\frac{c}{d}.$$

So, we have

$$y(x) = e^{-\frac{c}{d}\left(k_4\frac{x^2}{2}+k_3x\right)}\left(c_1 + \int -\frac{c}{d}e^{\frac{c}{d}\left(k_4\frac{x^2}{2}+k_3x\right)}dx\right)$$

$$= e^{-\frac{c}{d}\left(k_4\frac{x^2}{2}+k_3x\right)}\left(c_1 - \frac{\sqrt{c}}{\sqrt{d}\sqrt{k_4}}e^{-\frac{ck_3^2}{2dk_4}}\sqrt{\frac{\pi}{2}}\,\mathrm{erf}\left[\frac{\sqrt{c}}{\sqrt{2}}\frac{k_3+k_4x}{\sqrt{d}\sqrt{k_4}}\right]\right)$$

Now, remembering that $v = v_p + v_1 = 0 + v_1$ and $v_1 = y^{-1}$, we obtain the general solution for the first case as

$$v(x) = \frac{e^{\frac{c}{d}\left(k_4\frac{x^2}{2}+k_3x\right)}}{c_1 - \frac{\sqrt{c}}{\sqrt{d}\sqrt{k_4}}e^{-\frac{ck_3^2}{2dk_4}}\sqrt{\frac{\pi}{2}}\,\mathrm{erf}\left[\frac{\sqrt{c}}{\sqrt{2}}\frac{k_3+k_4x}{\sqrt{d}\sqrt{k_4}}\right]}.$$

Letting $v(0) = 2$, we have

$$2 = \frac{1}{c_1 - \frac{\sqrt{c}}{\sqrt{d}\sqrt{k_4}}e^{-\frac{ck_3^2}{2dk_4}}\sqrt{\frac{\pi}{2}}\,\mathrm{erf}\left[\frac{\sqrt{c}}{\sqrt{2}}\frac{k_3}{\sqrt{d}\sqrt{k_4}}\right]}.$$

Thus,

$$c_1 = \frac{1}{2} + \frac{\sqrt{c}}{\sqrt{d}\sqrt{k_4}} e^{-\frac{ck_3^2}{2dk_4}} \sqrt{\frac{\pi}{2}} \operatorname{erf}\left[\frac{\sqrt{c}}{\sqrt{2}} \frac{k_3}{\sqrt{d}\sqrt{k_4}}\right]$$

and remembering that in this case we chose $k_2 = 0$ we can substitute $\frac{k_1}{d}$ in k_4 since, by definition, $d > 0$ we obtain

$$c_1 = \frac{1}{2} + \frac{\sqrt{c}}{\sqrt{k_1}} e^{-\frac{ck_3^2}{2k_1}} \sqrt{\frac{\pi}{2}} \operatorname{erf}\left[\frac{\sqrt{c}}{\sqrt{2}} \frac{k_3}{\sqrt{k_1}}\right]$$

and

$$v(x) = \frac{e^{\frac{c}{d}\left(\frac{k_1 x^2}{2d} + k_3 x\right)}}{1/2 + \frac{\sqrt{c}}{\sqrt{k_1}} e^{-\frac{ck_3^2}{2k_1}} \sqrt{\frac{\pi}{2}} \left(\operatorname{erf}\left[\frac{\sqrt{c}}{\sqrt{2}} \frac{k_3}{\sqrt{k_1}}\right] - \operatorname{erf}\left[\frac{\sqrt{c}}{\sqrt{2}} \frac{k_3 + \frac{k_1}{d} x}{\sqrt{k_1}}\right]\right)}.$$

To find k_3 we can now use the condition we have on the derivative for $x = 0$ and the initial conditions: $\frac{\partial v}{\partial x}(0) = \frac{c}{d} u(0) v(0) = 2\frac{c}{d}$

To simplify notation of $v(x)$ we put

$$a(x) = \frac{c}{d}\left(\frac{k_1}{d} x + k_3\right),$$

$$A(x) = \int a(x) = \frac{c}{d}\left(\frac{k_1 x^2}{2d} + k_3 x\right),$$

$$B = -\frac{ck_3^2}{2k_1},$$

$$D(x) = 1/2 + \frac{\sqrt{c}}{\sqrt{k_1}} e^{-\frac{ck_3^2}{2k_1}} \sqrt{\frac{\pi}{2}} \left(\operatorname{erf}\left[\frac{\sqrt{c}}{\sqrt{2}} \frac{k_3}{\sqrt{k_1}}\right] - \operatorname{erf}\left[\frac{\sqrt{c}}{\sqrt{2}} \frac{k_3 + \frac{k_1}{d} x}{\sqrt{k_1}}\right]\right)$$

and we remember that

$$\frac{\partial(\operatorname{erf}[f(x)])}{\partial x} = \frac{2}{\sqrt{\pi}} e^{-f(x)^2} f'(x).$$

So

$$D' = -\left(\frac{\sqrt{c}}{\sqrt{k_1}} e^B \frac{\sqrt{\pi}}{\sqrt{2}} \frac{\sqrt{c}}{\sqrt{d}} e^{\frac{c\left(k_3 + \frac{k_1}{d} x\right)^2}{2k_1}} \sqrt{\frac{k_1}{d}} \sqrt{\frac{2}{\pi}}\right) =$$

$$= -\frac{c}{d} e^{\frac{c(dk_3+k_1x)^2}{2d^2k_1} - \frac{ck_3^2}{2k_1}},$$

$$v'(x) = \frac{a(x)e^{A(x)}D - e^{A(x)}D'}{D^2}$$

$$= \frac{a(x)e^{A(x)}D + e^{A(x)}\frac{c}{d}e^{\frac{c(dk_3+k_1x)^2}{2d^2k_1} - \frac{ck_3^2}{2k_1}}}{D^2}.$$

We note that

$$a(0) = \frac{c}{d}k_3,$$

$$A(0) = 0,$$

$$D(0) = 1/2.$$

Substituting all these constants, in a similar way as we saw for $u(x)$, we have:

$$v'(0) = \frac{\frac{c}{d}k_3 + \frac{c}{d}}{\frac{1}{4}} = 4\frac{c}{d}(k_3 + 1)$$

and

$$4\frac{c}{d}(k_3 + 1) = 2\frac{c}{d}.$$

Solving for k_3, we have

$$2k_3 + 2 = 1 \implies k_3 = -1.$$

Substituting the value of $k_3 = -1$ in $v(x)$:

$$v(x) = \frac{e^{\frac{c}{d}\left(\frac{k_1x^2}{2d} - x\right)}}{\frac{1}{2} + \frac{\sqrt{c}}{\sqrt{k_1}}e^{-\frac{c}{2k_1}}\sqrt{\frac{\pi}{2}}\left(\operatorname{erf}\left[\frac{\sqrt{c}}{\sqrt{2}}\frac{-1}{\sqrt{k_1}}\right] - \operatorname{erf}\left[\frac{\sqrt{c}}{\sqrt{2}}\frac{-1+\frac{k_1}{d}x}{\sqrt{k_1}}\right]\right)}.$$

The only parameter left is k_1. Again, normalising $v(x)$ over the domain gives k_1.
Let us now consider the second case.

Case 2: $\mathbf{v_p = \alpha}$, $\mathbf{k_4 = 0}$ and $\boldsymbol{\alpha} = \frac{\mathbf{-ck_3 \pm \sqrt{c^2k_3^2 - 4ck_2}}}{\mathbf{2c}}$

Again, $k_4 = 0$ means $k_1 = k_2$ and we found analogously to the case for $u(x)$ that $k_3 = -1$. Thus, the expression for α becomes:

$$\alpha = \frac{c \pm \sqrt{c^2 - 4ck_2}}{2c} \tag{A.5}$$

and the equation to solve is:

$$v' - \frac{c}{d}v = \frac{c}{d}v^2 + \frac{k_2}{d},$$

so we see that v_p satisfies it for construction.
A solution $v = v_1 + v_p$ implies that

$$v_1' + \frac{c}{d}(v_1 + \alpha) = \frac{c}{d}\left(\alpha^2 + v_1^2 + 2\alpha v_1\right) + \frac{k_2}{d}$$

$$v_1' - \frac{c}{d}(k_3 + 2\alpha)v_1 = \frac{c}{d}v_1^2$$

Now putting

$$y = v_1^{-1}$$

we have $y' = -\frac{v_1'}{v_1}$ and

$$y' + \frac{c}{d}(2\alpha - 1)y = -\frac{c}{d}$$

which is linear and still gives

$$y(x) = e^{-A(x)}\left(c_1 + \int f(x)e^{A(x)}\right)$$

where

$$A(x) = \int \frac{c}{d}(-1 + 2\alpha) = \frac{c}{d}(-1 + 2\alpha)x$$

and

$$f(x) = -\frac{c}{d}.$$

Thus,

$$y(x) = e^{-\frac{c}{d}(-1+2\alpha)x}\left(c_1 - \int \frac{c}{d}e^{\frac{c}{d}(-1+2\alpha)x}\right) = e^{-\frac{c}{d}(-1+2\alpha)x}\left(c_1 - \frac{e^{\frac{c}{d}(-1+2\alpha)x}}{-1 + 2\alpha}\right).$$

Remembering $y(x) = v_1^{-1}(x)$ and $v(x) = v_p(x) + v_1(x)$:

$$v(x) = \frac{(-1+2\alpha)e^{\frac{c}{d}(-1+2\alpha)x}}{(-1+2\alpha)c_1 - e^{\frac{c}{d}(-1+2\alpha)x}} + \alpha. \tag{A.6}$$

As per case 2 for $u(x)$, we can impose now the integral constraint on $v(x)$:

$$\begin{aligned}
1 &= \int_0^1 v(x)dx = \int_0^1 \frac{(-1+2\alpha)e^{\frac{c}{d}(-1+2\alpha)x}}{(-1+2\alpha)c_1 - e^{\frac{c}{d}(-1+2\alpha)x}} + \alpha dx = \\
&= \left[-\frac{d}{c}\log(c_1(-1+2\alpha) - e^{\frac{c}{d}(-1+2\alpha)x}) + \alpha x\right]_0^1 = \\
&= \frac{d}{c}\log(c_1(-1+2\alpha) - 1) - \frac{d}{c}\log\left(c_1(-1+2\alpha) - e^{\frac{c}{d}(-1+2\alpha)}\right) + \alpha,
\end{aligned}$$

which gives

$$1 = \frac{d}{c}\log\left(\frac{c_1(-1+2\alpha)-1}{c_1(-1+2\alpha) - e^{\frac{c}{d}(-1+2\alpha)}}\right) + \alpha$$

and allows us to solve for c_1:

$$\frac{c}{d}(1-\alpha) = \log\left(\frac{c_1(-1+2\alpha)-1}{c_1(-1+2\alpha) - e^{\frac{c}{d}(-1+2\alpha)}}\right)$$

$$e^{\frac{c}{d}(1-\alpha)} = \frac{c_1(-1+2\alpha)-1}{c_1(-1+2\alpha) - e^{\frac{c}{d}(-1+2\alpha)}}$$

$$c_1(-1+2\alpha) - 1 = e^{\frac{c}{d}(1-\alpha)}\left(c_1(-1+2\alpha) - e^{\frac{c}{d}(-1+2\alpha)}\right)$$

$$c_1(-1+2\alpha)(e^{\frac{c}{d}(1-\alpha)} + 1) = -1 + e^{\frac{c}{d}(-1+2\alpha)+\frac{c}{d}(1-\alpha)} = -1 + e^{\frac{c}{d}\alpha}$$

$$c_1 = \frac{-1+e^{\frac{c}{d}\alpha}}{(-1+2\alpha)(e^{\frac{c}{d}(1-\alpha)}+1)}.$$

Now we can substitute in (A.6) the expression for c_1:

$$v(x) = \frac{(-1+2\alpha)e^{\frac{c}{d}(-1+2\alpha)x}}{(-1+2\alpha)\frac{-1+e^{\frac{c}{d}\alpha}}{(-1+2\alpha)(e^{\frac{c}{d}(1-\alpha)}+1)} - e^{\frac{c}{d}(-1+2\alpha)x}} + \alpha. \tag{A.7}$$

Now the dependence is only on the parameter k_2, thus substituting the expression for α in (A.7) and imposing the constraint at the boundary

$$0 = \frac{c}{d}v(0)u(0) = 2\frac{c}{d}$$

we can obtain the explicit form of $v(x)$.
The last example is given by the following.

Case 3: $\mathbf{v_p = \alpha x + \beta}$ with $\boldsymbol{\alpha} = \frac{\mathbf{k_2}}{\mathbf{d}}$, $\boldsymbol{\beta} = -\mathbf{k_3}$ and $\mathbf{k_1 = 0}$

The particular solution becomes

$$v_p = \frac{k_2}{d}x - k_3,$$

and we have to solve

$$v' - \frac{c}{d}\left(-\frac{k_2}{d}x + k_3\right)v = \frac{c}{d}v^2 + \frac{k_2}{d}.$$

We search $v = v_1 + v_p$ that satisfies the equation above, knowing that even the particular solution satisfies the same equation:

$$v_1' + v_p' - \frac{c}{d}\left(-\frac{k_2}{d}x + k_3\right)(u_1 + u_p) = \frac{c}{d}(u_1^2 + u_p^2 + 2u_1u_p) + \frac{k_2}{d},$$

so

$$v_1' - \frac{c}{d}\left(-\frac{k_2}{d}x + k_3\right)v_1 = \frac{c}{d}\left(v_1^2 + 2v_1\left(-\frac{k_2}{d}x + k_3\right)\right),$$

$$v_1' + \frac{c}{d}\left(-\frac{k_2}{d}x + k_3\right)v_1 = \frac{c}{d}v_1^2.$$

Now we have $v_1^{-1} = y$ and so $y' = -\frac{v_1'}{v_1^2}$, hence:

$$-y' + \frac{c}{d}\left(-\frac{k_2}{d}x + k_3\right)y = \frac{c}{d}.$$

The equation

$$y' + \frac{c}{d}\left(\frac{k_2}{d}x - k_3\right)y = -\frac{c}{d}$$

has the same property of all others, so:

$$y(x) = e^{-A(x)}\left(c_1 + \int -f(x)e^{A(x)}dx\right)$$

where

$$A(x) = \int \frac{c}{d}\left(\frac{k_2}{d}x - k_3\right)dx = \frac{c}{d}\left(\frac{k_2}{d}\frac{x^2}{2} - k_3x\right)$$

and

$$f(x) = -\frac{c}{d}.$$

Mathematica suggests the solution

$$\begin{aligned} y(x) &= e^{-\frac{c}{d}\left(\frac{k_2}{2d}x^2 - k_3 x\right)} \left(c_1 - \int \frac{c}{d} e^{\frac{c}{d}\left(\frac{k_2}{2d}x^2 - k_3 x\right)} dx \right) = \\ &= e^{-\frac{c}{d}\left(\frac{k_2}{2d}x^2 - k_3 x\right)} \left(c_1 - \frac{\sqrt{c}}{\sqrt{k_2}} e^{-\frac{ck_3^2}{2k_2}} \sqrt{\frac{\pi}{2}} \operatorname{erfi}\left[\sqrt{\frac{c}{2}} \frac{-dk_3 + k_2 x}{d\sqrt{k_2}} \right] \right). \end{aligned}$$

Knowing that $y(x) = v_1^{-1}(x)$ and $v(x) = v_p(x) + v_1(x)$, we can find

$$v_1(x) = \frac{e^{\frac{c}{d}\left(\frac{k_2}{2d}x^2 - k_3 x\right)}}{c_1 - \frac{\sqrt{c}}{\sqrt{k_2}} e^{-\frac{ck_3^2}{2k_2}} \sqrt{\frac{\pi}{2}} \operatorname{erfi}\left[\sqrt{\frac{c}{2}} \frac{-dk_3 + k_2 x}{d\sqrt{k_2}} \right]},$$

$$v(x) = \frac{e^{\frac{c}{d}\left(\frac{k_2}{2d}x^2 - k_3 x\right)}}{c_1 - \frac{\sqrt{c}}{\sqrt{k_2}} e^{-\frac{ck_3^2}{2k_2}} \sqrt{\frac{\pi}{2}} \operatorname{erfi}\left[\sqrt{\frac{c}{2}} \frac{-dk_3 + k_2 x}{d\sqrt{k_2}} \right]} + \frac{k_2}{d}x - k_3.$$

Imposing the initial condition $v(0) = 2$ we obtain c_1 as follows:

$$2 = \frac{1}{c_1 - \frac{\sqrt{c}}{\sqrt{k_2}} e^{-\frac{ck_3^2}{2k_2}} \sqrt{\frac{\pi}{2}} \operatorname{erfi}\left[\sqrt{\frac{c}{2}} \frac{-k_3}{\sqrt{k_2}} \right]} - k_3$$

$$c_1(2 + k_3) = (2 + k_3) \left(\frac{\sqrt{c}}{\sqrt{k_2}} e^{-\frac{ck_3^2}{2k_2}} \sqrt{\frac{\pi}{2}} \operatorname{erfi}\left[\sqrt{\frac{c}{2}} \frac{-k_3}{\sqrt{k_2}} \right] \right) + 1$$

$$c_1 = \frac{\sqrt{c}}{\sqrt{k_2}} e^{-\frac{ck_3^2}{2k_2}} \sqrt{\frac{\pi}{2}} \operatorname{erfi}\left[\sqrt{\frac{c}{2}} \frac{-k_3}{\sqrt{k_2}} \right] + \frac{1}{2 + k_3}.$$

Finally we arrive at:

$$v(x) = \frac{e^{\frac{c}{d}\left(\frac{k_2}{2d}x^2 - k_3 x\right)}}{\frac{\sqrt{c}}{\sqrt{k_2}} e^{-\frac{ck_3^2}{2k_2}} \sqrt{\frac{\pi}{2}} \operatorname{erfi}\left[\sqrt{\frac{c}{2}} \frac{-k_3}{\sqrt{k_2}} \right] + \frac{1}{2+k_3} - \frac{\sqrt{c}}{\sqrt{k_2}} e^{-\frac{ck_3^2}{2k_2}} \sqrt{\frac{\pi}{2}} \operatorname{erfi}\left[\sqrt{\frac{c}{2}} \frac{-dk_3 + k_2 x}{+} d\sqrt{k_2} \right]} + \frac{k_2}{d}x - k_3$$

We can write $v'(x)$ to impose $v'(0) = 2\frac{c}{d}$ or $v'(0) = \frac{c}{d}(4 + 2k_3)$.

Using better notation:

$$v(x) = \frac{e^{A(x)}}{\frac{\sqrt{c}}{\sqrt{k_2}} e^{-\frac{ck_3^2}{2k_2}} \sqrt{\frac{\pi}{2}} \left(\text{erfi}\left[\sqrt{\frac{c}{2}} \frac{-k_3}{\sqrt{k_2}}\right] - \text{erfi}\left[\sqrt{\frac{c}{2}} \frac{-dk_3 + k_2 x}{d\sqrt{k_2}}\right]\right) + \frac{1}{2+k_3}} + \frac{k_2}{d} x - k_3 =$$

where

$$A(x) = \frac{c}{d}\left(\frac{k_2}{2d} x^2 - k_3 x\right),$$

$$a(x) = \frac{c}{d}\left(\frac{k_2}{d} x - k_3\right),$$

$$D(x) = \frac{\sqrt{c}}{\sqrt{k_2}} e^{-\frac{ck_3^2}{2k_2}} \sqrt{\frac{\pi}{2}} \left(\text{erfi}\left[\sqrt{\frac{c}{2}} \frac{-k_3}{\sqrt{k_2}}\right] - \text{erfi}\left[\sqrt{\frac{c}{2}} \frac{-dk_3 + k_2 x}{d\sqrt{k_2}}\right]\right) + \frac{1}{2+k_3},$$

$$D'(x) = -\frac{c}{d} e^{-\frac{ck_3^2}{2k_2} + \frac{c(-dk_3 + k_2 x)^2}{2d^2 k_2}}.$$

So

$$A(0) = 0 \to e^{A(0)} = 1,$$

$$a(0) = -\frac{c}{d} k_3,$$

$$D(0) = \frac{1}{2+k_3},$$

$$D'(0) = 0,$$

and

$$v'(x) = e^{A(x)} \frac{a(x)D(x) - D'(x)}{D^2(x)} + \frac{k_2}{d}.$$

We can impose the condition:

$$v'(0) = -\frac{c}{d} k_3 (2 + k_3) + \frac{k_2}{d},$$

and solve for k_2

$$\implies 2\frac{c}{d} = -\frac{c}{d} k_3 (2 + k_3) + \frac{k_2}{d}$$

$$k_2 = (ck_3(2 + k_3) + 2c).$$

This allows us to write an analytical expression for the more complex case:

$$v(x) = e^{\frac{c}{d}\left(\frac{(ck_3(2+k_3)+2c)}{2d}x^2 - k_3 x\right)} \Bigg/ \left(\frac{\sqrt{c}}{\sqrt{(ck_3(2+k_3)+2c)}} e^{-\frac{ck_3^2}{2(ck_3(2+k_3)+2c)}} \sqrt{\frac{\pi}{2}} \cdot \right. \tag{A.8}$$

$$\cdot \left(\text{erfi}\left[\sqrt{\frac{c}{2}} \frac{-k_3}{\sqrt{(ck_3(2+k_3)+2c)}} \right] - \text{erfi}\left[\sqrt{\frac{c}{2}} \frac{-dk_3 + (ck_3(2+k_3)+2c)x}{d\sqrt{(ck_3(2+k_3)+2c)}} \right] \right) +$$

$$\left. + \frac{1}{2+k_3} \right) + \frac{(ck_3(2+k_3)+2c)}{d} x - k_3.$$

This final expression will need to satisfy the normalisation condition, by imposing which we can find k_3.
One final observation is the following. We kept the solution as general as possible, trying to consider the expressions arising when the integration constants of the one-dimensional ODE are not specified. This does not guarantee that the solutions always have a sound biological meaning for every set of constants considered.

Appendix B

Examples of numerical algorithms used in this thesis

Let us present the most interesting functions implemented in MATLAB to describe the spatial distribution, in one dimensional domain, of two koalas starting from adjacent trees or from the same tree.
The functions can be divided in two parts: in the first, we integrate the equations to understand if the curves have an intersection with the x-axes, Then, we plot the solutions, taking into consideration the zeros of the function previously found. Thus, in the second part the problem becomes a multi-region boundary value problem and the functions differentiate depending on the region they are considering.

B.1 Initial guess

To solve our problem and enforce the right conditions and constraints, an initial guess is necessary. For most of the plots in this study we consider an exponential guess function as a starting expression. The same results are also given by a parabolic guess function. Functions need at least to satisfy the boundary conditions. Consider two different possibilities:

```
function g = guess_esponential(x)
   ug = exp(-x);          % ug(0)=1; decrease from left to right
   vg = 2 * exp(x-1);     % vg(1)=2; decrease from right to left
   upg = -exp(-x);        % u derivative
   vpg = 2 * exp(x);      % v derivative
   wg = ug*x;
   zg = vg*x;
```

```
   g = [ug; upg; vg; vpg; wg; zg];
end

function y = guess(x, c, d)
    ug = 1 - 0.5*x.^2;
    vg = 2 - 1.5*x.^2;
    upg = -x;
    vpg = -3*x;
    wg = ug*x;
    zg = vg*x;

    y = [ug; upg; vg; vpg; wg; zg];
end

function y = guess_multi(x, region, c, d)

    u0 = 1 - 0.5*x^2;
    v0 = 2 - 1.5*x^2;
    up0 = -x;
    vp0 = -3*x;
    w0 = x;
    z0 = x;

    if region == 2
        % v at zero
        v0 = 0; vp0 = 0; z0 = 1;
    elseif region == 3
        % u,v at zero
        u0 = 0; up0 = 0; w0 = 1;
        v0 = 0; vp0 = 0; z0 = 1;
    end

    y = [u0; up0; v0; vp0; w0; z0];
end
```

As the reader can see, a third function defined, differencing over different regions, is also a possibility.

B.2 Defining the ODE via odefun

This is one of the principal parts of the code. Here we impose the ordinary differential equations that define the problem.

```
function dydx = odefun(x,y,d,c,m,lambda)
        u = y(1);
        up= y(2);

        v = y(3);
        vp= y(4);

        p = u*(1 + m*v)/(1 - m^2*u*v); %u scent mark density
        q = v*(1 + m*u)/(1 - m^2*u*v); %v scent mark density

        pp=(up.*(1+m*v)+u.*m.*vp.*(1+m*u))./(1-m^2*u.*v).^2; %p'
        qp=(vp.*(1+m*u)+m.*v.*up.*(1+m*v))./(1-m^2*u.*v).^2; %q'

        dydx=zeros(6,1);

        dydx(1) = up;

        dydx(2) = c/d*(up*q+u*qp)+lambda(1); %d^2udx^2=c/d d(uq)dx+lambdau
        dydx(3) = vp;
        dydx(4) = c/d*(vp*p+pp*v)+lambda(2); %d^2vdx^2=c/d d(pv)dx+lambdav

        dydx(5) = u ;
        dydx(6) = v ;

end


function dydx = odefun_multi(x, y, region, d, c, m, lambda)
    u = y(1); up = y(2); v = y(3); vp = y(4);
    dydx = zeros(6,1);

    if region == 1
        %u,v>0

        p = u*(1+m*v)/(1 - m^2*u*v);
        q = v*(1+m*u)/(1 - m^2*u*v);
```

```
        pp = ((up*(1+m*v) + u*m*vp)*(1 - m^2*u*v) + p*m^2*(up*v + u*vp))/...
             (1 - m^2*u*v)^2;
        qp = ((vp*(1+m*u) + m*v*up)*(1 - m^2*u*v) + q*m^2*(up*v + u*vp))/...
                (1 - m^2*u*v)^2;

        dydx(1) = up;
        dydx(2) = (c/d)*(up*q + u*qp) + lambda(1);
        dydx(3) = vp;
        dydx(4) = (c/d)*(vp*p + pp*v) + lambda(2);
        dydx(5) = u; dydx(6) = v;

    elseif region == 2
        %u>0, v=v'=0
        den = max(1 - m^2*u*v, 1e-4);
        p = u*(1+m*v)/den; q = v*(1+m*u)/den;
        common = m^2*(up*v + u*vp);
        pp = ((up*(1+m*v) + u*m*vp)*den + p*common) / den^2;
        qp = ((vp*(1+m*u) + m*v*up)*den + q*common) / den^2;

        dydx(1) = up;
        dydx(2) = (c/d)*(up*q + u*qp) + lambda(1);
        dydx(3) = 0;
        dydx(4) = 0;
        dydx(5) = u; dydx(6) = 0;

    else
        % assume derivate=0 to maintain u e v a 0
        dydx = zeros(6,1);
    end
end
```

Again, depending on the guess, which in turn depends on the parameters of the condition chosen, different expressions are considered. The equations are then numerically integrated via the MATLAB routine, defining two auxiliary variables, $w := \int u(x)dx$ and $z = \int v(x)dx$, such that $w_1 = 1,\ w_0 = 0,\ z_1 = 1$ and $z_0 = 0$ to enforce the integral constraints. Furthermore, an unknown two-dimensional parameter lambda is introduced to provide the necessary degree of freedom for the solver to satisfy all conditions imposed in the bcfun.

B.3 Boundary, integral conditions and constraints

The built-in conditions typical of the problem are collated in bcfun. First of all, we impose u and v having a chosen fixed point ($u(0) = 1$ and $v(0) = 2$) and the boundary Neumann conditions. Thus, the flux at the boundary should be zero, in particular here we impose only $u_0' - \frac{c}{d}u_0v_0 = 0$ and $v_0' - \frac{c}{d}u_0v_0 = 0$ but it should be same imposing the condition on x=1.

```
    function res = bcfun(ya,yb,d,c,m,lambda)
        u0 = ya(1); up0=ya(2); v0 = ya(3); vp0=ya(4);
        u1 = yb(1); up1=yb(2); v1 = yb(3); vp1=yb(4);

        w0 = ya(5);  z0 = ya(6);
        w1 = yb(5);  z1 = yb(6);


        p0 = u0*(1 + m*v0)/(1 - m^2*u0*v0);
        q0 = v0*(1 + m*u0)/(1 - m^2*u0*v0);
        p1 = u1*(1 + m*v1)/(1 - m^2*u1*v1);
        q1 = v1*(1 + m*u1)/(1 - m^2*u1*v1);


        % Constraints and conditions:
        res = [ u0 - 1;     % u(0)=1
                v0 - 2      % v(0)=2
                up0-c/d*u0*q0;    %u0'-c/d*u0*q0=0
                vp0-c/d*v0*p0     %v0'-c/d*v0*p0=0
                w0;
                z0;
                w1-1;
                z1-1];

end


    function res = bcfun_front(ya, yb, d, c, m, lambda)

    res = [
        % --- (x=0) [4 conditions] ---
        ya(1,1) - 1;          % u(0) = 1
```

```
        ya(3,1) - 2;          % v(0) = 2
        ya(5,1);
        ya(6,1);

        % --- (x=x1, v=0 at x1) [6 conditions] ---
        yb(3,1);
        yb(1,1) - ya(1,2);
        yb(2,1) - ya(2,2);
        %yb(4,1)-ya(4,2);
        yb(3,1) - ya(3,2);
        yb(5,1) - ya(5,2);
        yb(6,1) - ya(6,2);

        %  (x=x2, u=0 at x2) [6 conditions]
        yb(1,2);
        yb(1,2) - ya(1,3);
        yb(2,2) - ya(2,3);
        yb(3,2) - ya(3,3);
        yb(5,2) - ya(5,3);
        yb(6,2) - ya(6,3);

        % (x=1) [4 conditions]
        yb(5,3) - 1;
        yb(6,3) - 1;
        yb(2,3);
        yb(4,3)
    ];
end
```

Various different conditions are expressed, depending on "where" on the interval they must be applied. The integrals for $u(x)$ and $v(x)$ are given by variables w_1 and z_1.
Finally, let us briefly describe how we integrate the PDE. To numerically solve the system of PDEs, we implemented the pdepe solver in MATLAB. This solver requires two functions that describe the PDE system and the initial condition. We define the initial condition using two Dirac Delta functions, representing the initial presence of the two koalas at specific locations; in particular, in Figs. 3.2-3.4, we consider one delta function centred at x=0.05, corresponding to the Koala U, and the other centred at x=0.99, representing

the koala V. To define the main function that represents the system it is required to write the PDEs in the following form:

$$c\left(x,t,u,\frac{\partial u}{\partial t}\right)\frac{\partial u}{\partial t}=\frac{\partial}{\partial x}\left(f\left(x,t,u,\frac{\partial u}{\partial x}\right)\right)+s\left(x,t,u,\frac{\partial u}{\partial x}\right).$$

In our model, $c=[1;1]$, $s=[0;0]$ and the flux term is defined as

$$f=[D\frac{\partial u}{\partial x}-Cqu;\ D\frac{\partial v}{\partial x}-Cpv]$$

where p and q represent the densities of the scent mark of U and V, respectively.
Furthermore, we define two vectors x and t to specify the spatial and temporal step of the calculations. Both vectors were defined with linspace using 3000 points from 0 to 1, for x, and 300 points from 0 to 10, for t. It is worth noting that the underlying solver "pdepe" uses a fixed step for spatial mesh, but an adaptive step for the temporal domain. This is useful, specifically in our case during the initial phase where there are narrow deltas, which require numerical stability.

Bibliography

Wolgang Alt. Biased random walk models for chemotaxis and related diffusion approximations. *Journal of mathematical biology*, 9(2):147–177, 1980.

Douglas A Brown and Howard C Berg. Temporal stimulation of chemotaxis in escherichia coli. *Proceedings of the National Academy of Sciences*, 71 (4):1388–1392, 1974.

SM De Oliveira, PJ Murray, DL De Villiers, and GS Baxter. Ecology and movement of urban koalas adjacent to linear infrastructure in coastal south-east queensland. *Australian Mammalogy*, 36(1):45–54, 2014.

Natasha Ellison, Ben J Hatchwell, Sarah J Biddiscombe, Clare J Napper, and Jonathan R Potts. Mechanistic home range analysis reveals drivers of space use patterns for a non-territorial passerine. *Journal of Animal Ecology*, 89(12):2763–2776, 2020.

P Holgate. Random walk models for animal behavior. statistical ecology: Sampling and modeling biological popidations and population dynamics, volume 2 of penn state statistics, 1971.

Peter M Kareiva and Nanako Shigesada. Analyzing insect movement as a correlated random walk. *Oecologia*, 56(2):234–238, 1983.

Scott A Lassau, Brendan Ryan, Robert Close, Chris Moon, Pascal Geraghty, Ann Coyle, and John Pile. Home ranges and mortality of a roadside koala phascolarctos cinereus population at bonville, new south wales. *Australian Zoologist*, 34:127–136, 2008.

Gregory W Lollback, J Guy Castley, Alexa C Mossaz, and Jean-Marc Hero. Fine-scale changes in spatial habitat use by a low-density koala population in an isolated periurban forest remnant. *Australian Mammalogy*, 40(1):84–92, 2018.

Alison Matthews, Daniel Lunney, Shaan Gresser, and Wendy Maitz. Movement patterns of koalas in remnant forest after fire. *Australian Mammalogy*, 38(1):91–104, 2016.

Paul R Moorcroft and Mark A Lewis. *Mechanistic home range analysis.(MPB-43)*. Princeton University Press, 2006.

Akira Okubo, Simon A Levin, et al. *Diffusion and ecological problems: modern perspectives*, volume 14. Springer, 2001.

Eirikur Palsson and Hans G Othmer. A model for individual and collective cell movement in dictyostelium discoideum. *Proceedings of the National Academy of Sciences*, 97(19):10448–10453, 2000.

Roger Peters and L David Mech. Scent-marking in wolves. In *Wolf and Man*, pages 133–147. Elsevier, 1978.

Stephen Phillips. Aversive behaviour by koalas (phascolarctos cinereus) during the course of a music festival in northern new south wales, australia. *Australian Mammalogy*, 38(2):158–163, 2016.

Jonathan R Potts and Mark A Lewis. How memory of direct animal interactions can lead to territorial pattern formation. *Journal of the Royal Society Interface*, 13(118), 2016.

Darcy Watchorn. 'i was shocked': a scientist tracking koalas films startling behaviour between young males. *The Conversation*, 2025.

Darcy J Watchorn and Desley A Whisson. Quantifying the interactions between koalas in a high-density population during the breeding period. *Australian Mammalogy*, 42(1):28–37, 2019.